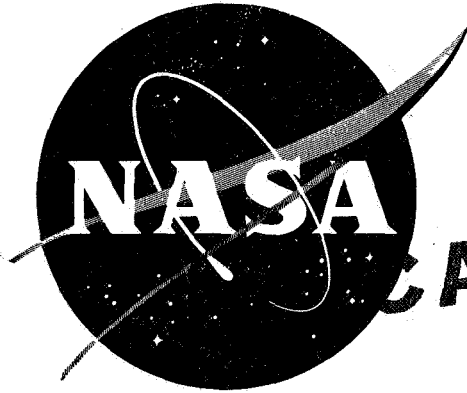NASA CASE FILE COPY

INVESTIGATION INTO THE MECHANISM OF DEGRADATION OF SOLAR CELLS WITH SILVER-TITANIUM CONTACTS

D2-126194-1

FIRST QUARTERLY PERIODIC PROGRESS REPORT

PREPARED FOR NATIONAL AERONAUTICS AND
SPACE ADMINISTRATION
WASHINGTON, D.C.
CONTRACT NO. NASW-1859

THE BOEING COMPANY, AEROSPACE GROUP, KENT FACILITY
SEATTLE, WASHINGTON

D2-126194-1

FIRST QUARTERLY PERIODIC PROGRESS REPORT
FOR
INVESTIGATION INTO THE MECHANISM OF
DEGRADATION OF SOLAR CELLS WITH
SILVER-TITANIUM CONTACTS
(1 APRIL 1969 - 30 JUNE 1969)
CONTRACT NO. NASW-1859

NASA HEADQUARTERS
CONTRACTING OFFICER: W. M. Collins, Jr.

Prepared by:
THE BOEING COMPANY
AEROSPACE GROUP
SEATTLE, WASHINGTON

TECHNICAL LEADER: W. F. Springgate
PROGRAM MANAGER: Henry Oman

FOR
NATIONAL AERONAUTICS AND SPACE ADMINISTRATION
WASHINGTON, D.C.

TABLE OF CONTENTS

ILLUSTRATIONS

1.0 SUMMARY

Degraded and undegraded solar cells were subjected to X-ray diffraction, mass spectroscopy, and internal reflectance spectroscopy during the first quarter of work at Boeing on Contract NASW-1859. Degradation has been observed under controlled laboratory conditions in solar cells exposed to electrolytic solutions and to high humidity. Important findings were:

o   Potentiostatic and rest-potential measurements confirmed that the degradation is electrochemical.

o   Rest potential determines whether a solar cell under electrolyte will or will not degrade in the manner that it degrades in a humid atmosphere.

o   Optical and electron photomicrographs show what appear to be grain boundaries. However, under higher resolution these grain boundaries resolve into grain plateaus.

o   Mass spectroscopy shows the presence of several contaminants which are important in other corrosion reactions. These include fluorides, copper, and water.

o   X-ray diffraction studies show the effect of sintering, i.e., a partially crystalline structure on the silver surface and an unidentified compound at the silver-titanium interface.

Two degradation mechanisms are being studied in detail. One relates the corrosion to capillary movement of moisture through the silver to react with titanium. The second postulates the transport of atomic hydrogen to an impervious boundary where $2H^o \rightarrow H_2$ forms a blister.

2.0 INTRODUCTION

This document (Ref. 1) describes work performed at Boeing during the first three months of NASA-Headquarters Contract NASW-1859, "Investigation into the Mechanism of Degradation of Solar Cells with Silver-Titanium Contacts."

The program is directed by Arvin H. Smith, Office of Advanced Research and Technology, National Aeronautics and Space Administration, Washington, D.C.

The contract duration is nine months. Many production silicon solar cells with silver-titanium contacts have degraded in time under normal atmospheric conditions. Degradation is manifested in two ways: (1) the appearance of small blisters, and (2) a decrease in the cell output as the voltage-current (V-I) curve under illumination flattens out.

The objective of this contracted work is to determine the fundamental mechanism which causes solar cells with silver-titanium contacts to degrade when exposed to a humid atmosphere. The work plan includes these tasks: (1) conduct a theoretical analysis of the electrochemical and physical mechanisms of the degradation; (2) conduct experiments to verify the theoretical analysis; (3) determine what steps in the manufacture of solar cells could produce residual contaminants; and (4) survey work done by other organizations that have information applicable to the problem.

3.0 TECHNICAL ACHIEVEMENTS

Boeing work during the first 3-month period of this study has produced two theoretical models for humidity degradation of solar cells. In one, blister-forming hydrogen generated by reaction with contaminants at the silver surface migrates through the silver lattice. In the other, water migrates through pores in the silver to react with titanium at the silver-titanium interface. Electrochemical, humidity, and physical tests have been directed toward verifying the theoretical models.

The tests have produced excellent quantitative results which, when incorporated into further theoretical analyses, have produced clear direction for the next quarter's activity.

The following subsections describe the theoretical models, the experimental work, and the unanswered questions. In Section 4.0 are recorded steps in the manufacture of solar cells. Conclusions are in Section 5.0. The work for the next quarter is described in Section 6.0.

3.1 THEORETICAL MODELS

Corrosion is an electrochemical process which needs a conductive solution in order to proceed. Two problems become evident:

1) How does the conductive solution form?

2) What are the electrochemical reactions involved in the corrosion process?

Two theoretical models are being studied in detail to explain the degradation of solar cell contacts. Model I involves reactions with contaminants at the silver surface with subsequent migration of the reaction products through the silver layer to the region of the silver-titanium contact, resulting in blistering and degradation. Previous work by others indicates that the blistering originates at the silver-titanium interface (Ref. 2 and 3). Model II assumes that water condenses in the pores in the silver layer and that the hydrogen-forming reaction takes place at the silver-titanium interface.

MODEL I - Hydrogen Diffusion---Blistering of metals has been encountered at Boeing with 7000-Series aluminum alloys. This occurs most frequently in the winter when moisture is a problem. Hydrogen appears to be the cause of blistering. If the protective oxide film of aluminum is broken by mechanical deformation or by chemical reaction with such agents as sulfur, ammonia, or chlorides, the fresh aluminum surface absorbs the atomic hydrogen liberated from local decomposition of water. When the diffusing hydrogen atoms arrive at a discontinuity such as a grain boundary, the hydrogen collects and recombines as molecular (diatomic) hydrogen. The hydrogen pressure builds up until blistering occurs.

The aluminum corrosion model suggests a solar-cell contact degradation mechanism. Water reacting with contaminants on the surface of the silver releases atomic hydrogen which subsequently migrates through the silver to the silver-titanium contact where boundaries cause the hydrogen atoms to collect and combine into hydrogen gas, forming blisters.

This model, if valid, would resolve the question of how the hydrogen can get into the volume where blistering starts, yet not escape as pressure builds up.

Model II - Titanium Corrosion---Model II assumes that the degradation is caused by the corrosion of titanium. Titanium metal normally forms a protective oxide coating which effectively separates the pure metal from the outside environment. However, if this coating is not present or is broken the titanium will corrode rather quickly. This model postulates that capillary condensation in the silver-titanium interface provides the conductive solution needed for corrosion. The size of the capillaries needed to condense water at various humidities can be calculated using the Kelvin equation: (Ref. 4)

$$RT \ln P/P_o = 2\gamma V/r$$

where:

R = gas constant = 8.314×10^7 erg/deg mole

T = absolute temperature, ^oK (298° for room temperature)

P = vapor pressure of water in pore, mm Hg

P_o = vapor pressure of water on flat surface, mm Hg

(P/P_o = relative humidity at which condensation will occur in a pore of radius r)

γ = surface tension, dyne/cm = 72.0 for water

V = molar volume, cm^3/mole (18.0 for H_2O)

r = pore radius, cm

This equation shows that at 50 percent relative humidity a pore-size of $30\overset{o}{A}$ will result in capillary condensation. The nature of the equation is such that a higher humidity value will produce condensation in smaller pores, and at lower relative humidities only larger pore diameters can act as condensation wells. Since a distribution of pore sizes can be anticipated, capillary condensation would well be expected over a range of humidity values.

Recent experiments have produced electron micrographs showing a grain-like structure in the evaporated silver (Ref. 5). The same experiments showed that the grain size is inversely related to the resistance to degradation at high humidities, i.e., smaller grain size giving better degradation resistance. Other experiments indicate transport through a porous silver layer to the titanium surface (Ref. 3). The exact mechanism of transport is not yet known (Ref. 6).
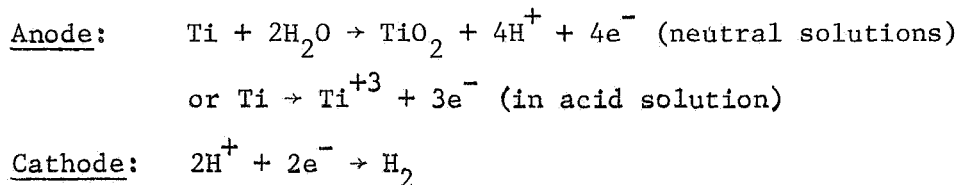
3.2 CONSTANT POTENTIAL TESTS

Our first laboratory work has been in producing controlled degradation of the solar cell contacts and determining the reaction mechanisms responsible for the degradation. Solar cells were exposed to various environments and their behavior was characterized. Several types of chemical and physical tests were performed.

The silicon solar cells used in these tests were Heliotek N-on-P type with a resistivity of 1 to 3 Ω cm. They were 2 by 2 cm size and 8 mils thick.

Although solar cells do degrade in humid air, the natural process is too slow for practical testing. We hoped to accelerate degradation by exposing the solar cells to specific chemical solutions and potentials under reproducible controlled conditions.

The electrochemical corrosion of titanium may be a cause of contact degradation. Possible reactions are:

$\underline{\text{Anode:}}$ $\quad$ $Ti + 2H_2O \rightarrow TiO_2 + 4H^+ + 4e^-$ (neutral solutions)

$\quad\quad\quad$ or $Ti \rightarrow Ti^{+3} + 3e^-$ (in acid solution)

$\underline{\text{Cathode:}}$ $\quad$ $2H^+ + 2e^- \rightarrow H_2$

The presence of H_2 in blisters (Ref. 5) is consistent with the above cathode reaction.

Contaminating ions can accelerate the process by breaking the oxide coating on the titanium or by chemically entering the reaction (e.g., Ti forms a stable complex with F^- at low pH values). We hope to determine the reaction mechanism by testing cells in various chemical solutions at different pH values. Various chemical species are thermodynamically stable depending on the pH of the solution. Figures 1 and 2 (Ref. 7) show the potential -pH diagrams for the silver-water and titanium-water systems at 25°C, and indicate regions where various species exhibit stable characteristics. Lines a and b refer to the boundaries for H_2 and O_2 reduction. Above a, the reaction $2H^+ + 2e^- \rightarrow H_2$ is thermodynamically impossible. Above b, the reaction $4H^+ + O_2 + 4e^- \rightarrow 2H_2O$ is impossible. For the titanium-water system the region of interest is bounded approximately by potentials of +0.2 volts and -1.2 volts at a pH of -1, and -0.8 volts and -2.2 volts at a pH of 14.
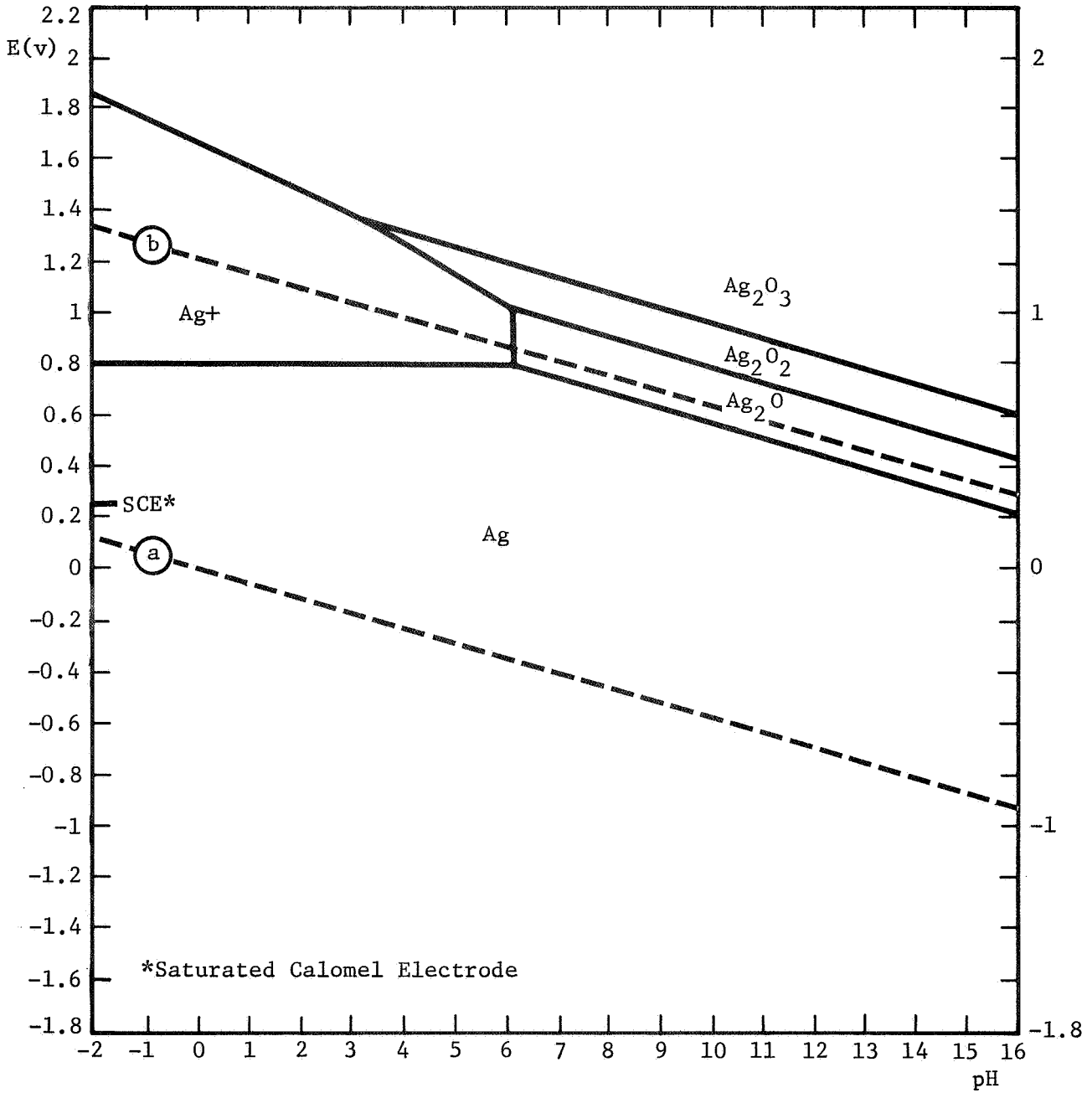
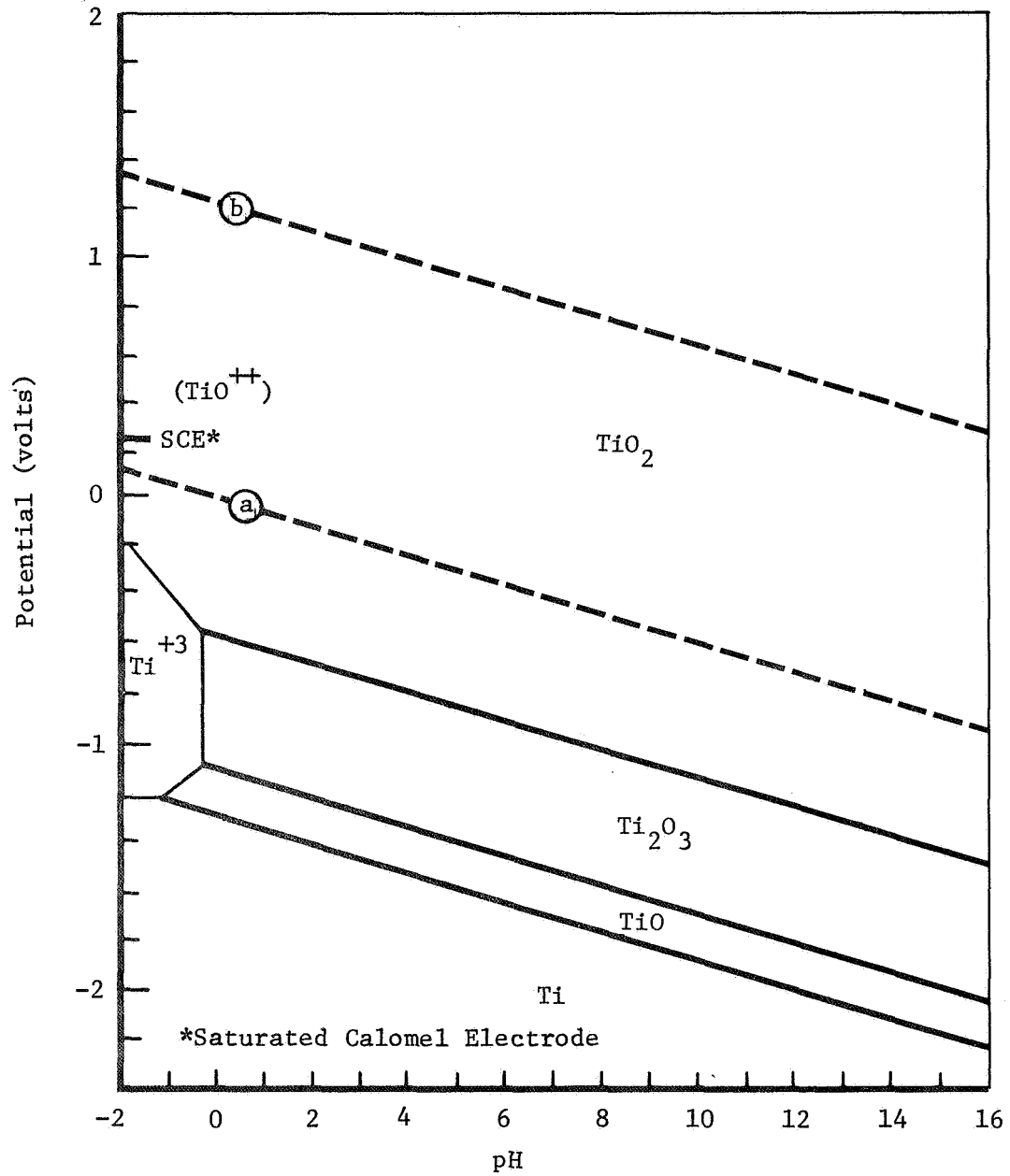Figure 1:   pH VERSUS POTENTIAL FOR SILVER-WATER SYSTEM AT 25° C

Figure 2:   pH VERSUS POTENTIAL FOR TITANIUM-WATER SYSTEM AT 25° C

Solutions of one normal HCl, H_2SO_4, NaCl, NaOH, and Na_2SO_4 were chosen
to provide electrolytes with a wide range of pH values and several
different ionic species. The pH of the solutions as measured with a
Beckman pH meter (model G) are:

Solution	pH
HCl	0.0
H_2SO_4	0.25
NaCl	7.23
NaOH	12.02
H_2O (boiled + deionized)	7.00

We had to apply potentials to the electrodes in order to study the sys-
tems as a function of potential and to learn about the reaction mecha-
nisms in terms of polarization or overpotential of the electrodes. The
solar cell, acting as the control electrode, was placed in a Teflon cell
filled with the appropriate solution (Figures 3 and 4). A platinum wire
served as the counter electrode and a saturated calomel reference
electrode (SCE) (Figure 5) was used. A Magna Potentiostat (Model 4700M)
was used to measure the current as a function of applied potential.

Potential varied as a sawtooth function of time applied to the cells
produced the polarization curve for IN HCl shown in Figure 6. The area
labeled "A" corresponds to cathodic behavior of the cell where the
reaction is $2H^+ + 2e^- \rightarrow H_2$. In area "B" the cell becomes anodic and
silver oxidizes to give silver chloride by the reaction $Ag + Cl^- \rightarrow$
$AgCl + e^-$. Region "C" corresponds to the reduction of the species oxidized
in region "B" ($AgCl + e^- \rightarrow Ag + Cl^-$). The shapes of regions "B" and "C" are
expected to vary as functions of the past history of the cell. The polar-
ization curves indicate the irreversibility of an electrode process.

A reference voltage-current (V-I) curve was recorded for each cell
before any electrochemical tests were performed with the cell. Figure 7
shows a typical V-I curve for an undegraded solar cell taken while the
cell was illuminated with simulated space sunlight from an Xenon lamp.
The potentiostatic tests were continued and V-I curves were periodically
obtained until degradation occurred. Solar cells in IN HCl solutions at
potentials of 0.0V and -0.3V with respect to a SCE reference electrode
degraded in 51 hours and 84 hours respectively, indicating that environ-
ment accelerates degradation. It is significant that applying a poten-
tial between the electrolyte and the silver-titanium contact of the
solar cell produces degradation at room temperature. The V-I curves
show how electrochemical conditions affect degradation. Figure 8
shows severe degradation occurring after 51 hours at a potential of
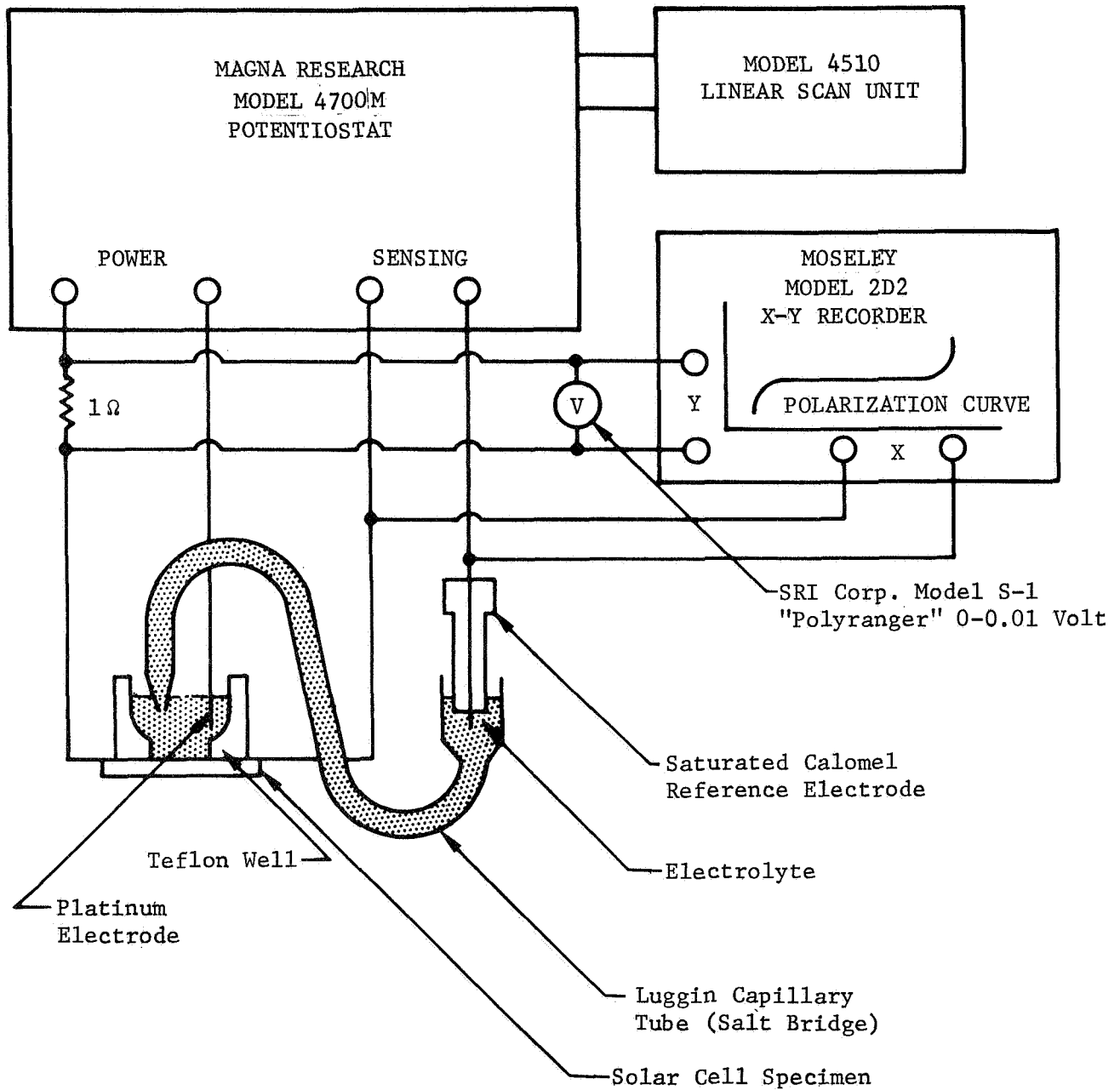0.0 volts in one-normal HCl. Somewhat less degradation occurred when

8
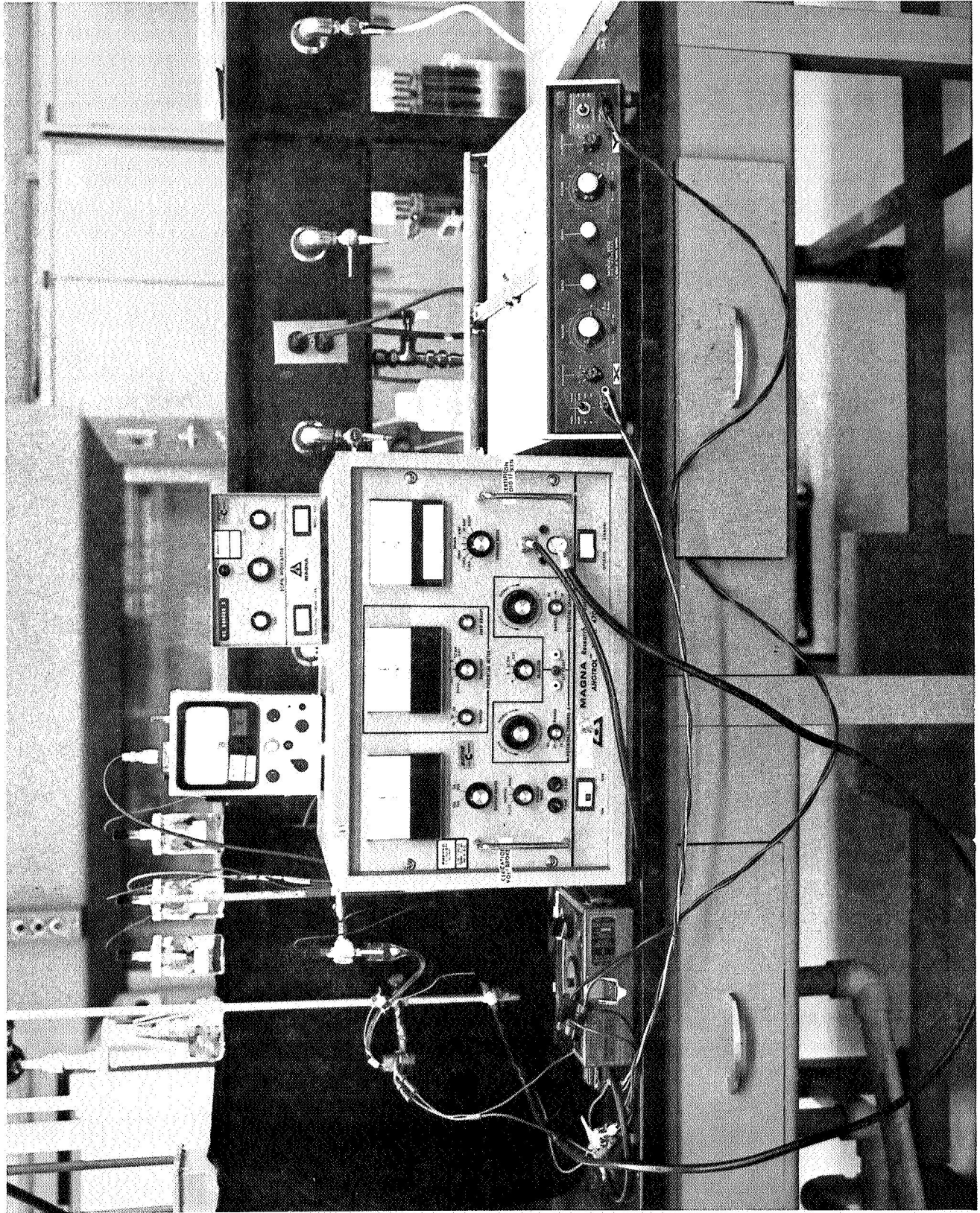
Figure 3: CONSTANT POTENTIAL APPARATUS

Figure 4: POTENTIOSTATIC TEST SETUP
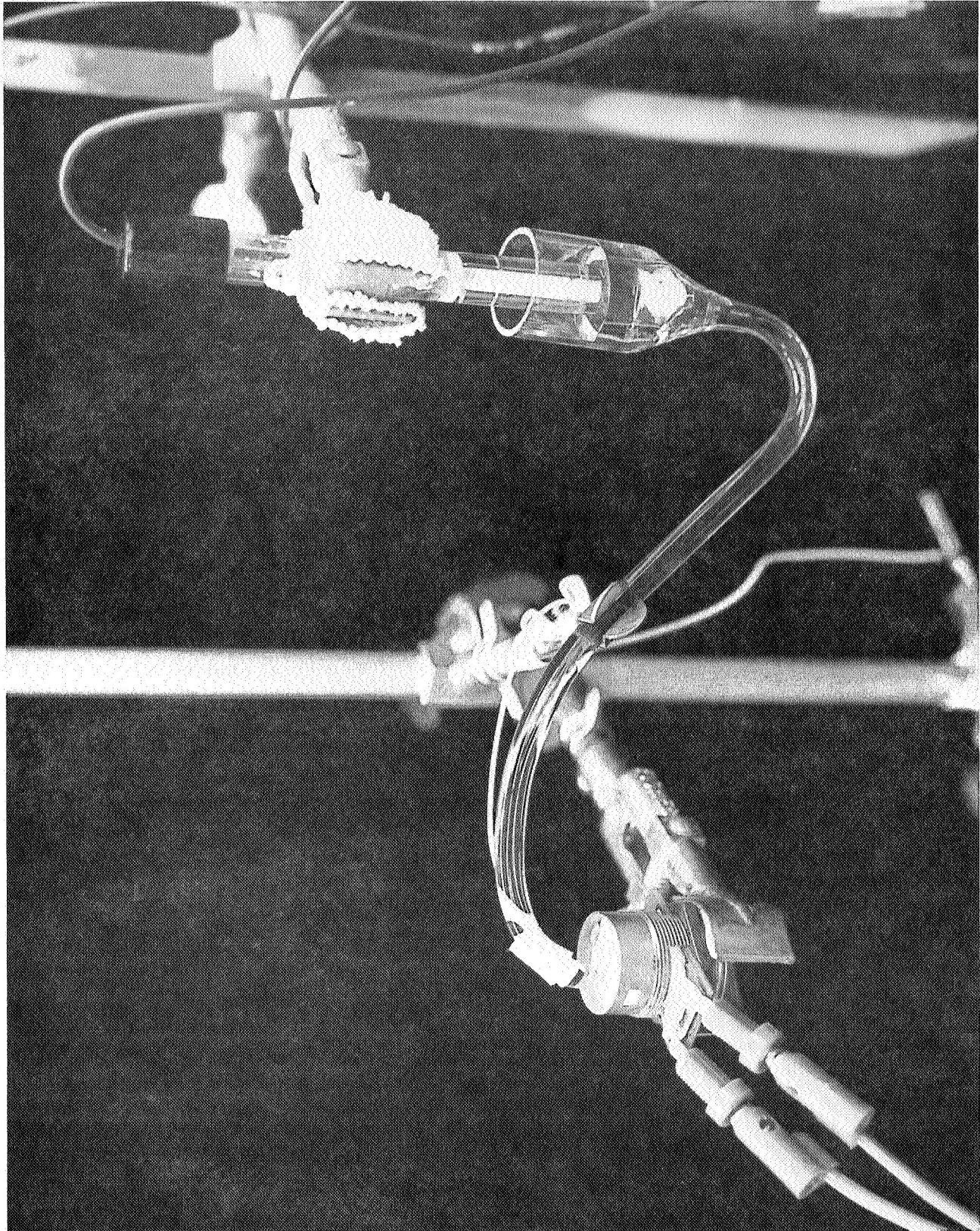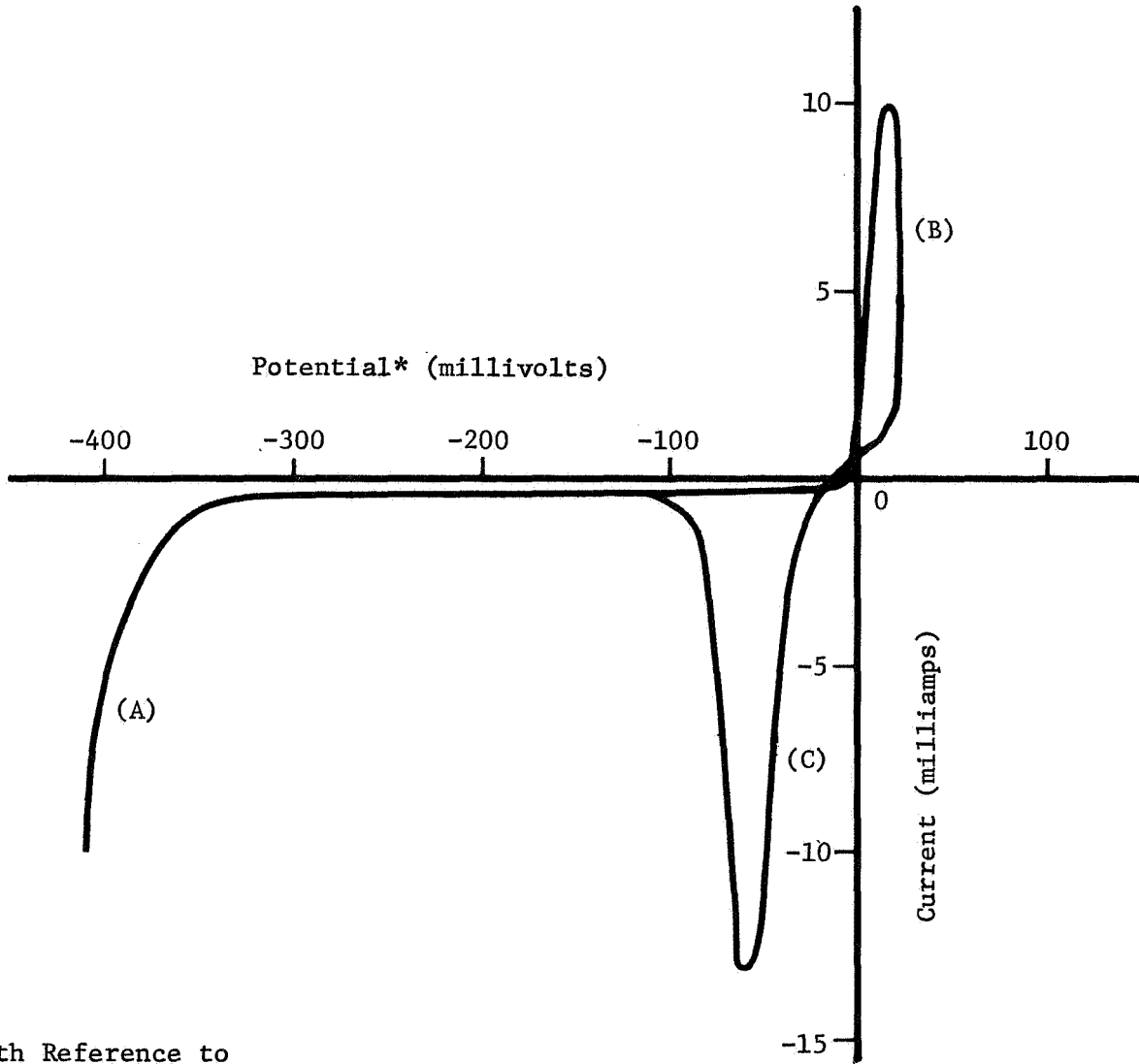
Figure 5:   SPECIMEN HOLDER, LUGGIN CAPILLARY, AND REFERENCE CALOMEL ELECTRODE

Specimen: Cell No. 115
Electrolyte: HCl
Solution: 1 Normal
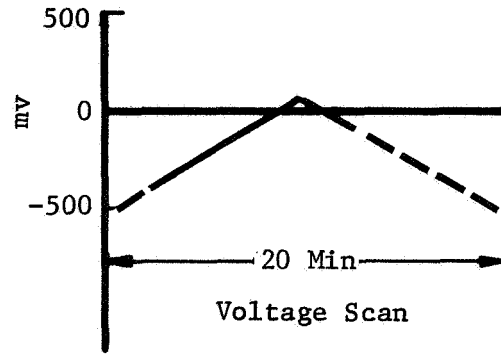
Figure 6:   HCl POLARIZATION CURVE

*With Reference to
 Saturated Calomel Electrode

V-I Characteristics

Solar Cell No. 88
Illumination
  Source: Xenon Lamp
  Intensity: 100 mw/cm^2
Temp: 28°C

Cell No. 88
Type: N on P Silicon
Size: 2 x 2 cm
Thickness: 8 mil
Base Resistivity: 1 ohm cm
Contact: Silver-Titanium
Mfr: Heliotek

Figure 7: TYPICAL UNDEGRADED PERFORMANCE OF A SOLAR CELL

Figure 8:   PERFORMANCE DEGRADATION FROM HCl AT 0.0 VOLTS

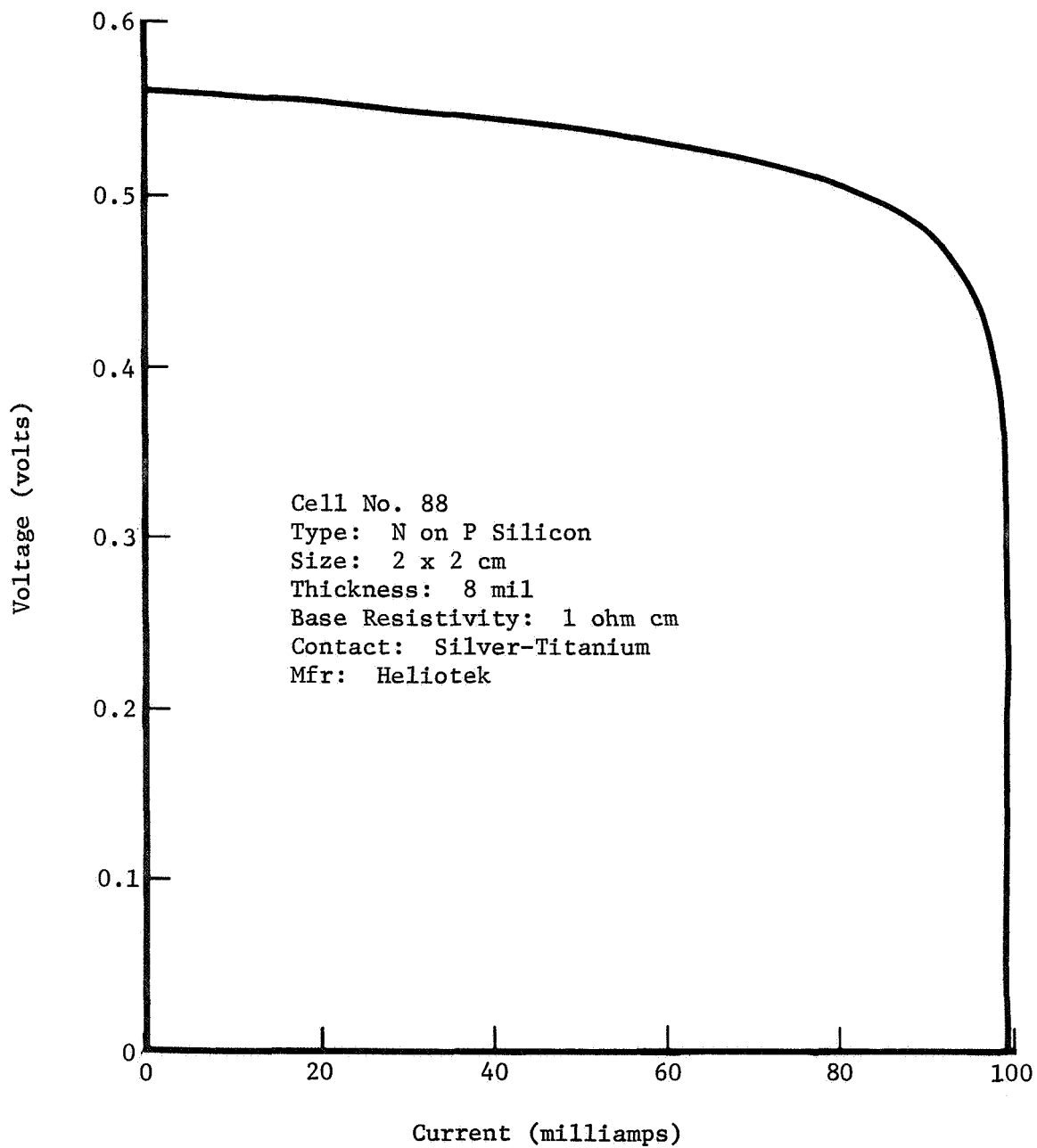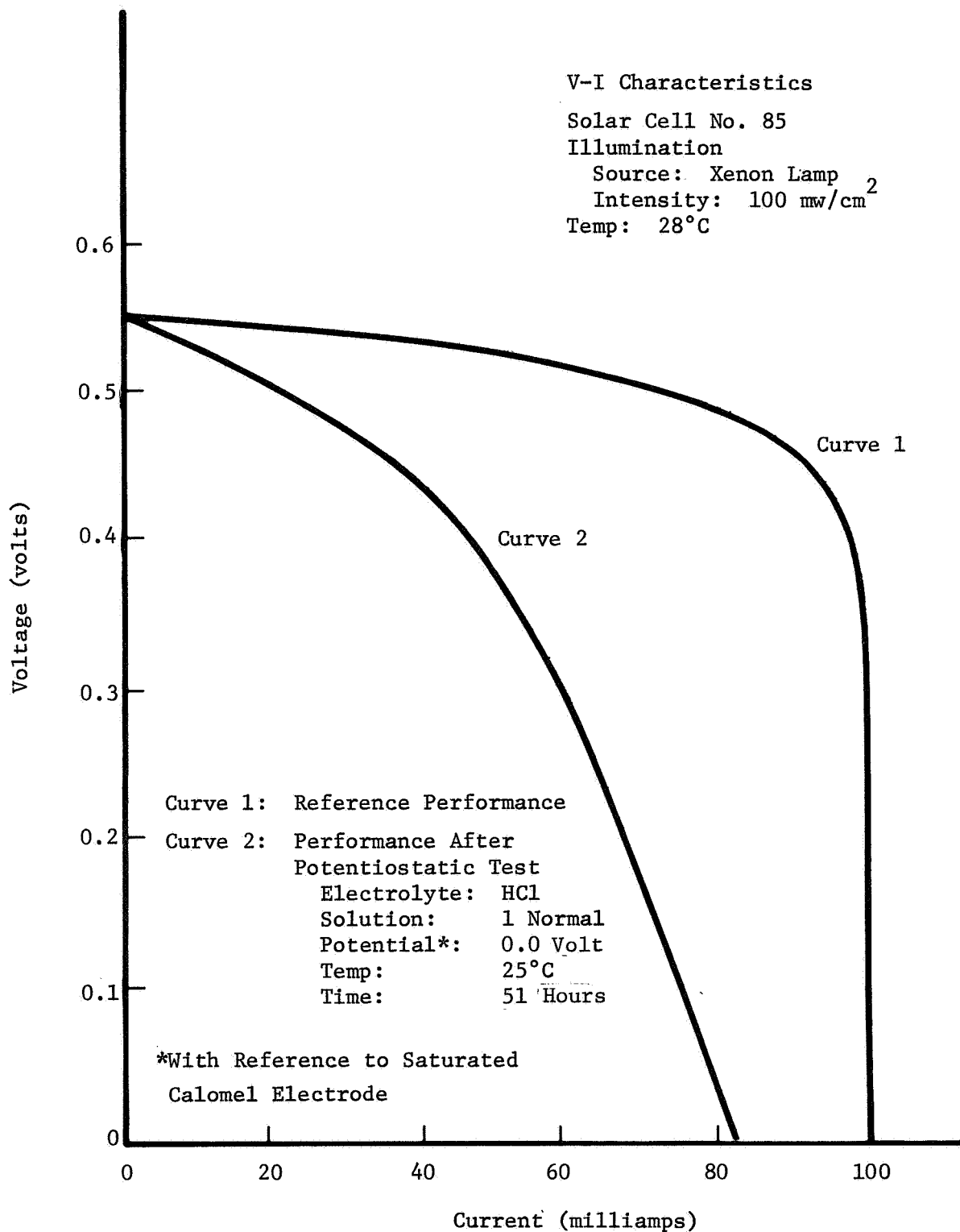the potential was maintained at -0.3 volts (Figure 9). A photograph of the blistered cell is shown in Figure 10. Cell power as a function of time was determined from the V-I curves (Figure 11). The steady decrease in power indicates that degradation is a continuing process.

The polarization curve of a degraded cell (Figure 12) has a shape similar to the curve obtained before degradation took place, but the potential at which the cell becomes cathodic has dropped from -0.4 volts to -0.25 volts. This implies a change in hydrogen overpotential.

The rest potential of the solar cell-HCl couple is negative, approximately -0.1 volts for most test cells. This indicates, that under anodic conditions, degradation is more rapid than under cathodic conditions. If titanium corrosion is responsible for the degradation, this result is contrary to what would be expected. A more positive potential is expected to passivate titanium and inhibit corrosion. More experimentation is necessary to resolve this problem. Similar tests are being planned for the solutions mentioned previously and others as the need arises.

3.3 REST POTENTIALS

Rest potential is the open circuit equilibrium potential which an electrochemical cell exhibits when its electrodes are in contact with the electrolyte. Rest potential versus time measurements, in addition to potentiostatic measurements, are being used to characterize the corrosion in the solar-cell contacts. The instrumentation required is not elaborate and several cells can be tested at the same time. Rest potentials are measured with a high impedance voltmeter (KEITHLEY, Model 200B) against a SCE reference electrode (Figure 13).

The electrolytes used were 1-normal solutions of HCl, NaOH, Na_2SO_4, NaCl, NH_4F and H_2SO_4. Deionized and boiled water was used as a control.

Figure 14 shows rest potentials as a function of time. These data, when considered with other solar-cell power degradation measurements, show that the negative rest potentials with respect to the SCE are associated with rapid degradation at room temperature and blistering. Of particular interest are the curves for the halides, because mass spectrographic analyses have shown a surprising amount of fluorides present on the solar cell surface (See Section 3.5, Physical Measurements). The fluorides seem to be a residue of the etching and cleaning processes used in the manufacture of the solar cells.

The rest potential of a pure silver electrode in the 1-normal solutions was measured for comparison purposes. The values were:

V-I Characteristics

Solar Cell No. 83
Illumination
  Source: Xenon Lamp
  Intensity: 100 mw/cm^2
Temp: 28°C

Curve 2

Curve 1

Voltage (volts)

Curve 1:   Reference Performance

Curve 2:   Performance After
           Potentiostatic Test
              Electrolyte: HCl
              Solution: 1 Normal
              Potential*:   -0.3 Volt
              Temp: 25°C
              Time: 84.5 Hours

*With Reference to Saturated Calomel Electrode
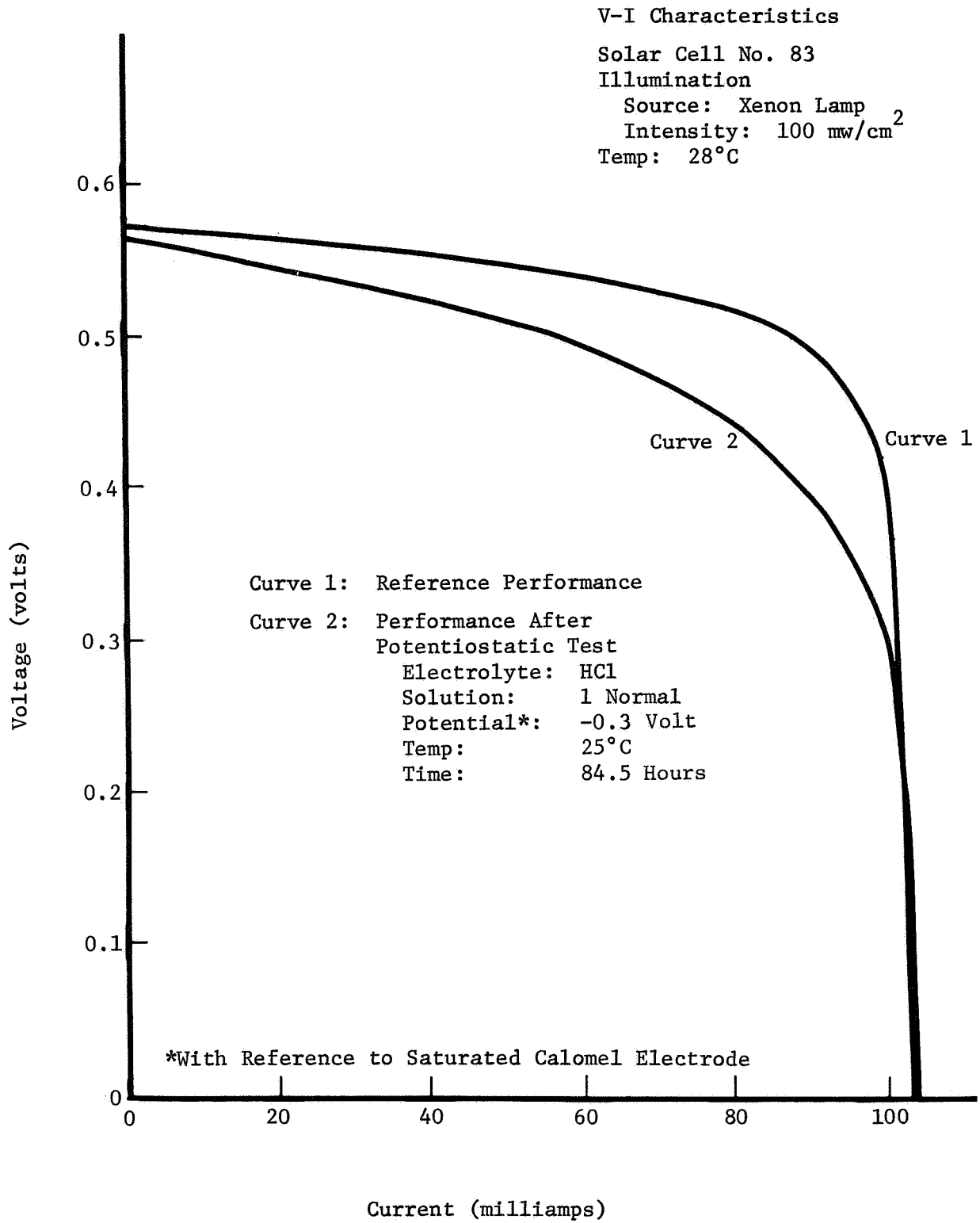
Current (milliamps)

Figure 9:   PERFORMANCE DEGRADATION FROM HCl AT -0.3 VOLTS
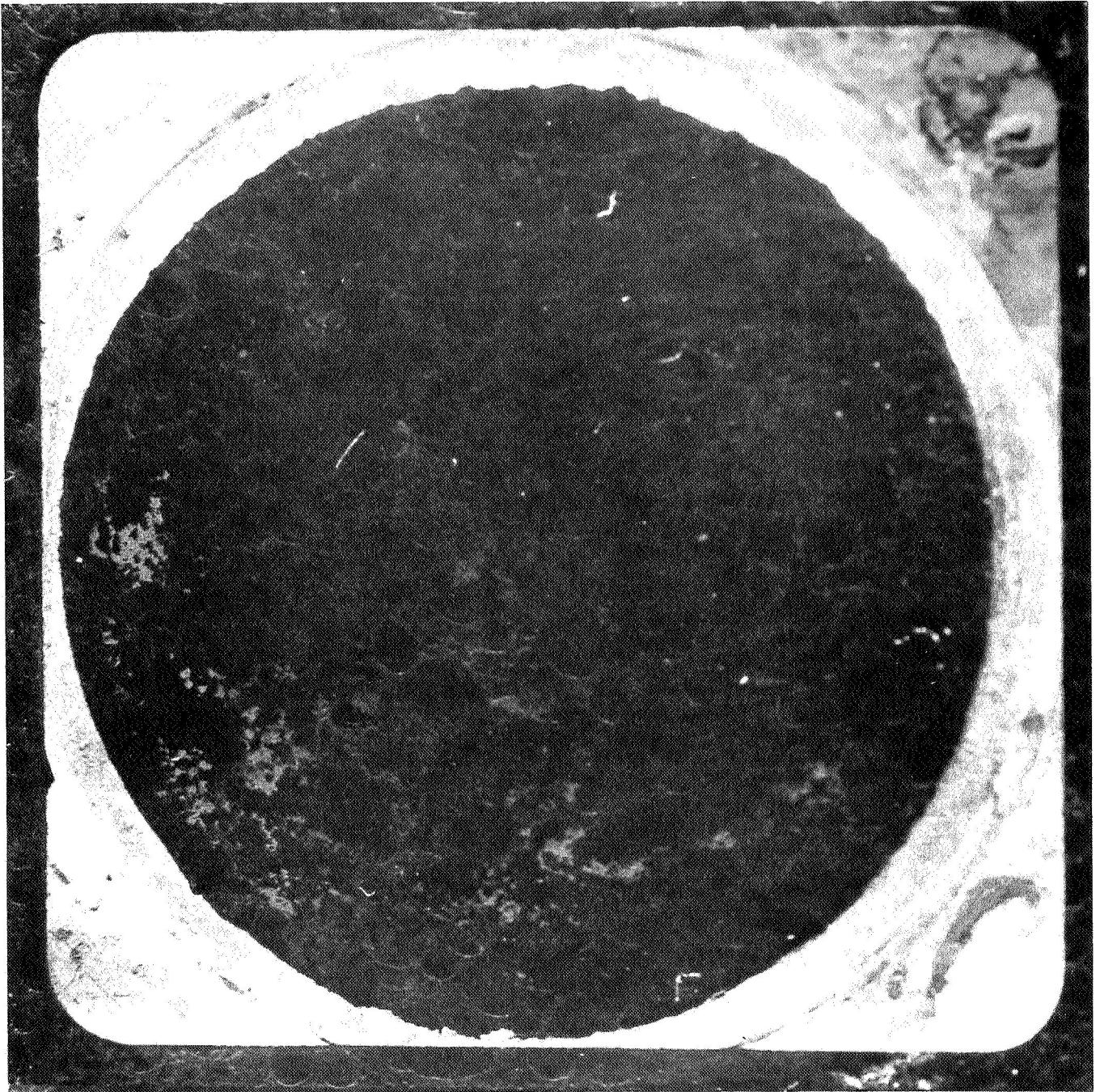
Figure 10:   SOLAR CELL AFTER 84 HOURS IN HCl AT -0.3 VOLTS

TIME	MAX. PWR.	
(HOURS)	(MW)	(%)
0	44.2	100
5.5	43.3	97.9
12.5	43.2	97.8
84.5	35.2	79.6

Specimen: Cell 83

Electrolyte: HCl

Solution: 1 Normal

Potential*: -0.3 Volt

Temp: 25°C

*With Reference to Saturated Calomel Electrode
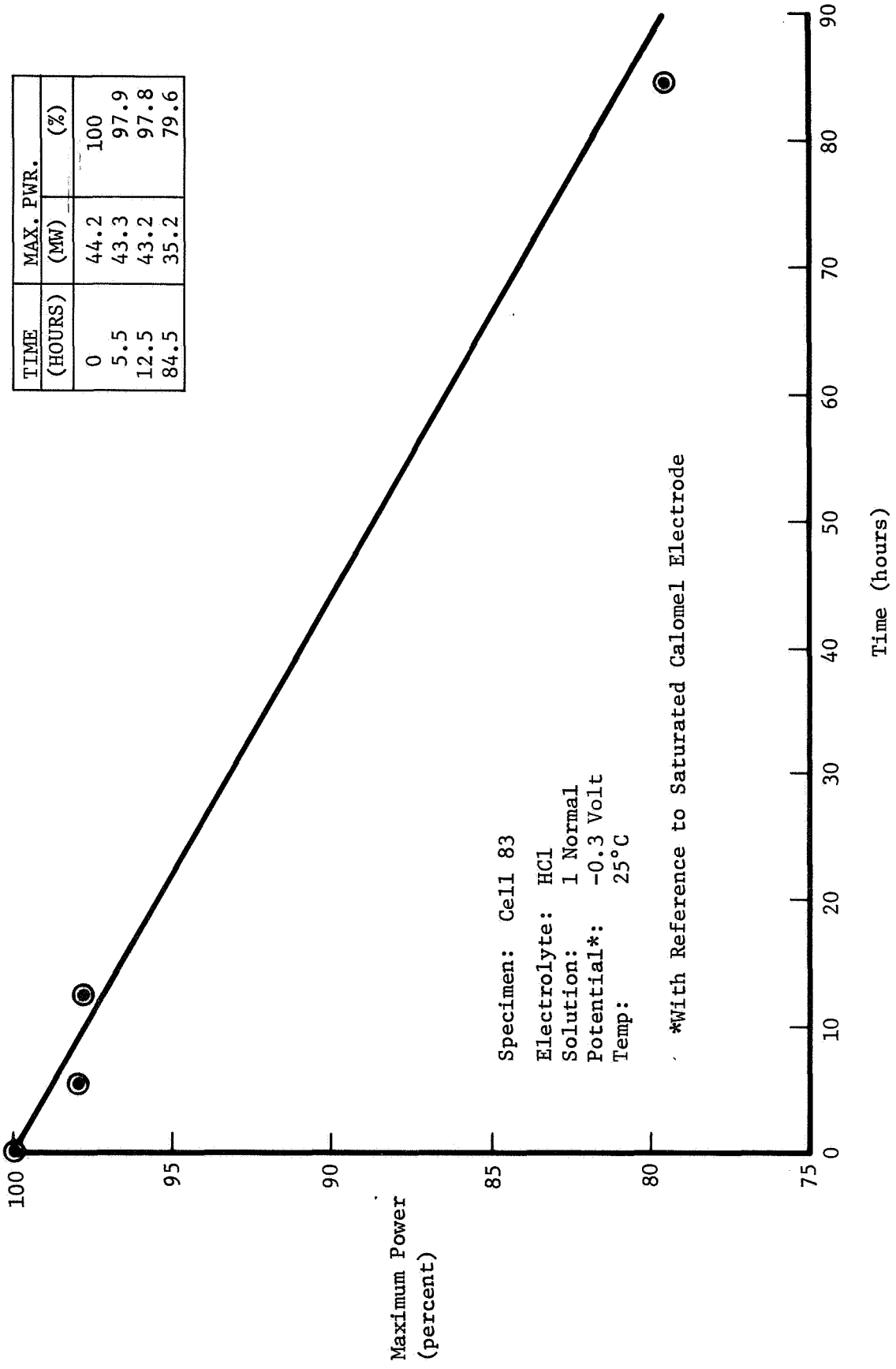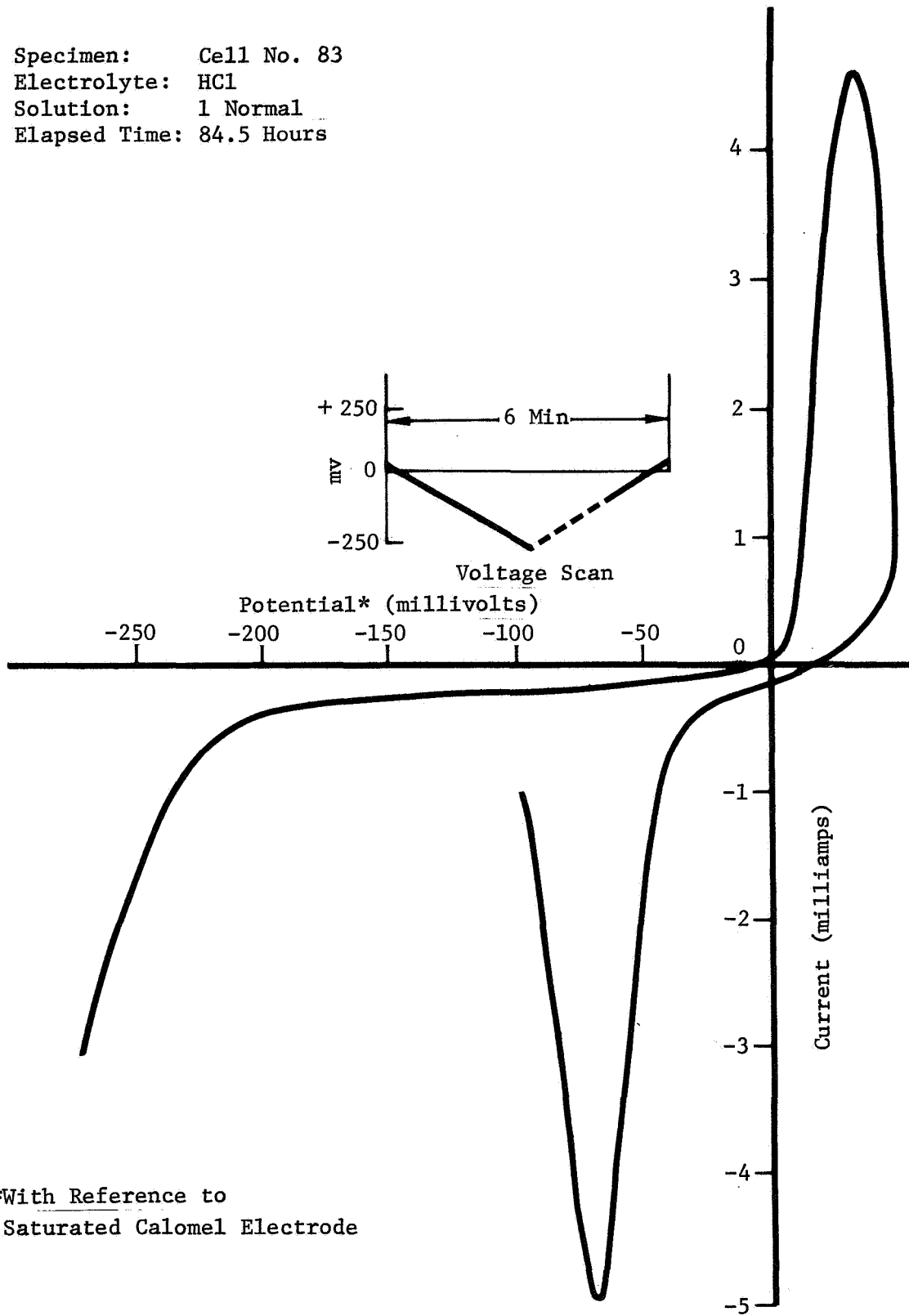
Maximum Power (percent)

Time (hours)

Figure 11: PERFORMANCE DEGRADATION RATE FROM HC1 AT 0.0 VOLTS

Specimen: Cell No. 83
Electrolyte: HCl
Solution: 1 Normal
Elapsed Time: 84.5 Hours

Figure 12:   HCl POLARIZATION CURVE AFTER 84 HOURS AT -0.3 VOLTS

Keithley
Model 200B
d.c. VTVM

Beckman Fiber
Junction Saturated
Calomel Reference
Electrode

Alligator
Clip

Test Cell
(2 x 2 cm)
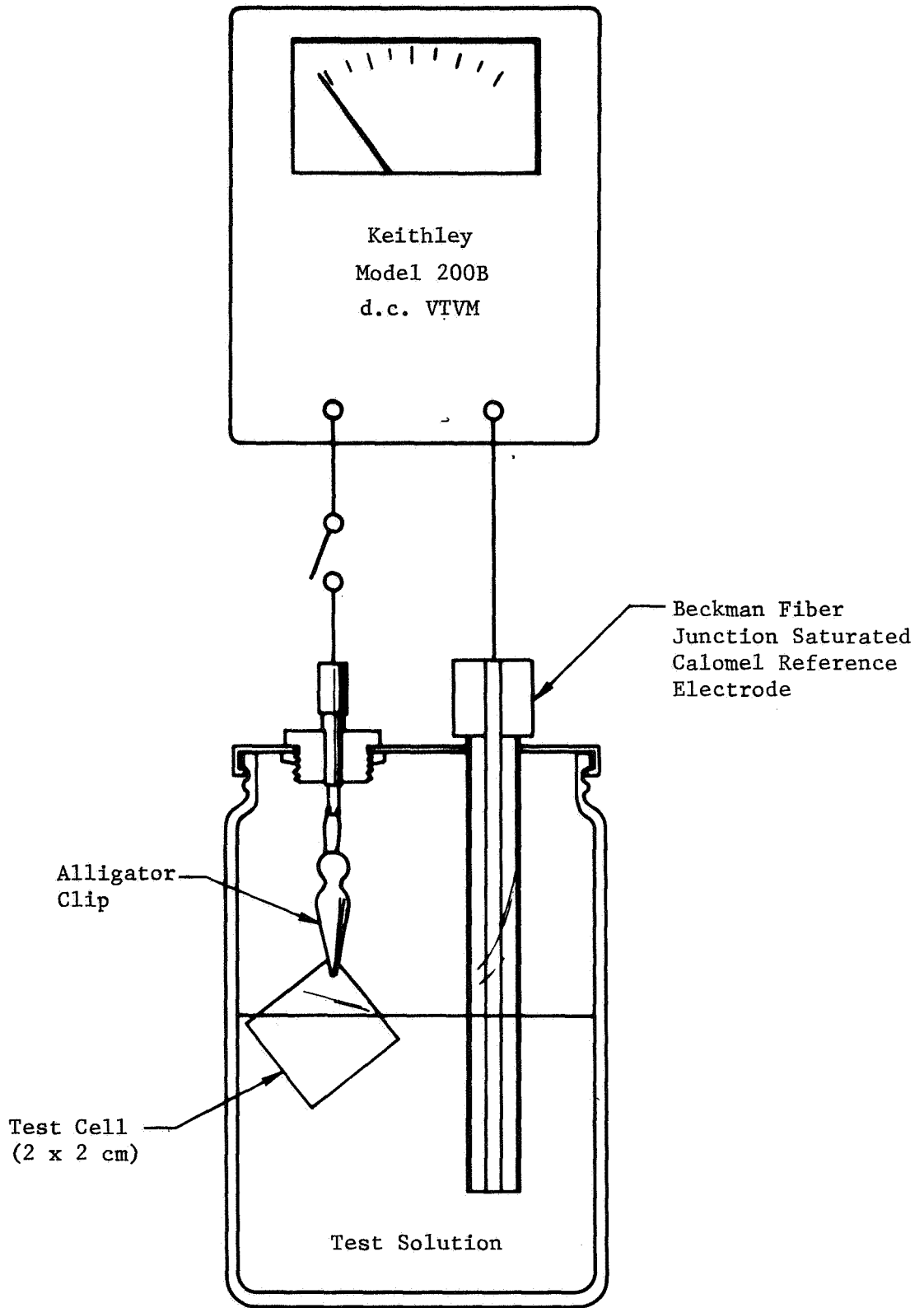
Test Solution

Figure 13:   REST POTENTIAL TEST SETUP
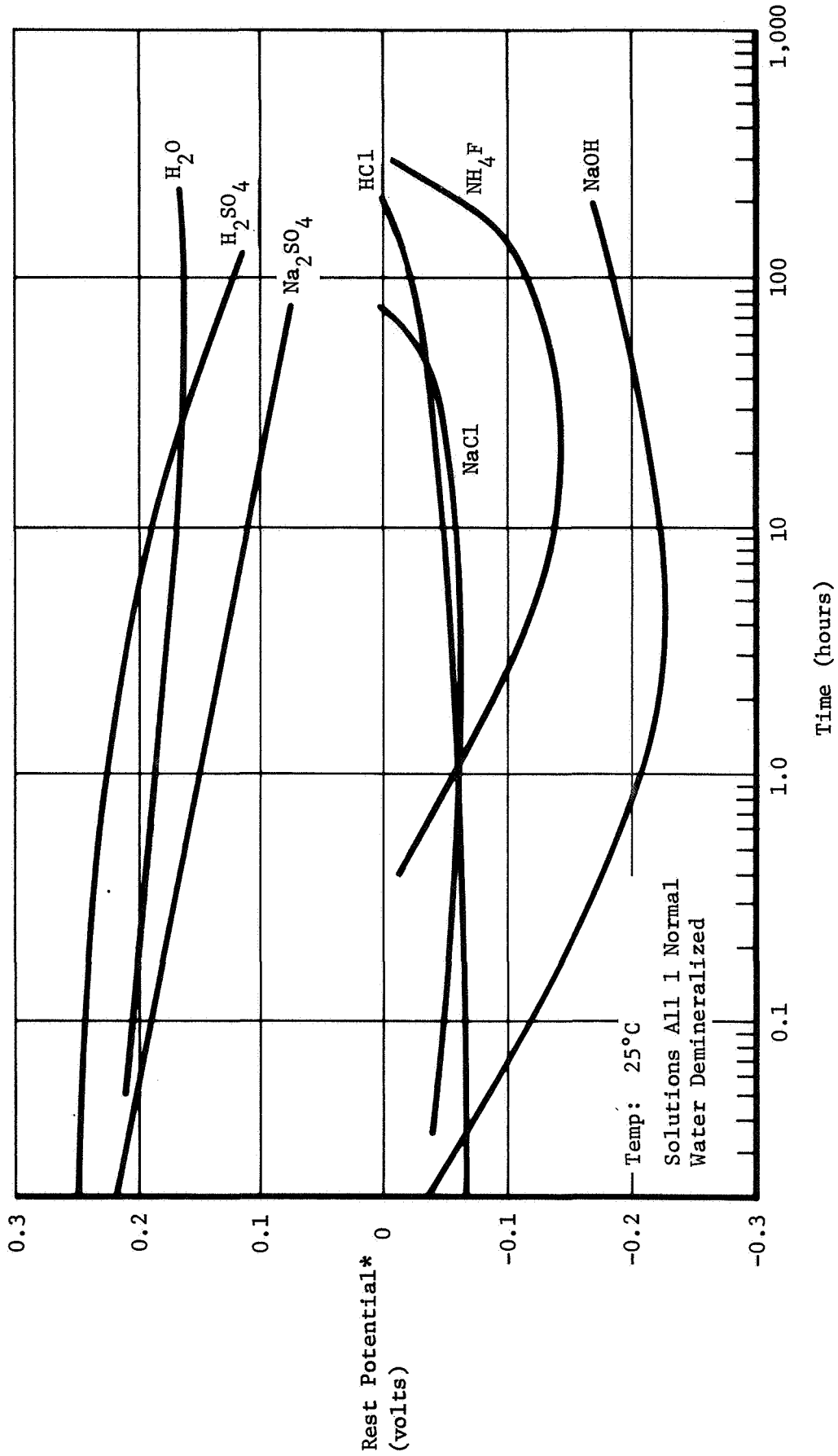
Figure 14: REST POTENTIAL* VERSUS TIME

*With Reference to Saturated Calomel Electrode

Solution	Probable Reaction	E_{Ag}	$E_{solar\ cell}$
1N HCl	$Ag + Cl^- \rightarrow AgCl + e^-$	+0.02V	-0.06V
1N H_2SO_4	$2Ag + SO_4^= \rightarrow Ag_2SO_4 + 2e^-$	+0.1V	+0.23V
1N NaOH	$2Ag + 2OH^- \rightarrow Ag_2O + H_2O + 2e^-$	-0.1V	-0.21V

The HCl and NaOH solutions, which result in similar degradation, produce in solar cells rest potentials which are lower than those for pure silver. This suggests a mixed potential resulting from an interaction with a substance, perhaps titanium, having a more negative rest potential. $SO_4^=$, which does not promote degradation, generates in solar cells a higher rest potential than it generates in silver. Rest potential measurements may provide a useful indicator of contact stability.

3.4 EFFECT OF HALOGENS

Chloride and other halogens ions are a possible cause of titanium corrosion. Chloride ions break down passivity in metals such as (Fe and Cr) by penetrating oxide layers (Ref. 8). The reaction is local rather than over the entire surface, and preferred sites are determined by variations in the oxide film. The hypothesis that halogens promote degradation was tested by storing solar cells in an atmosphere of water and HCl. The solar cells were above the water in a covered container having a relative humidity of 100 percent in a 90°C oven. After 75 hours the cell exhibited blisters and the V-I curves indicated that degradation had occurred. Figure 15 shows typical V-I curves before and after storage. A photograph of the degraded cell is shown in Figure 16.

Blisters similar to those obtained in the water humidity test became prominent after 6.5 hours of exposure when a solar cell was suspended over a concentrated 12-normal solution of HCl at room temperature. Shown in Figure 17 are V-I curves taken before exposure and after 68 hours of exposure to this HCl atmosphere. The degradation was severe (Figure 19). The corresponding power curve is shown in Figure 18. 3M found similar results with similar tests (Ref. 9).

The extent and type of degradation is apparently the same as occurs in an environment of 100 percent relative humidity at 90°C. The degradation rates can be related using an equation derived from Arrenhius' reaction rate theory:

$$\frac{R_2}{R_1} = 2^{(T_2 - T_1)/k}$$
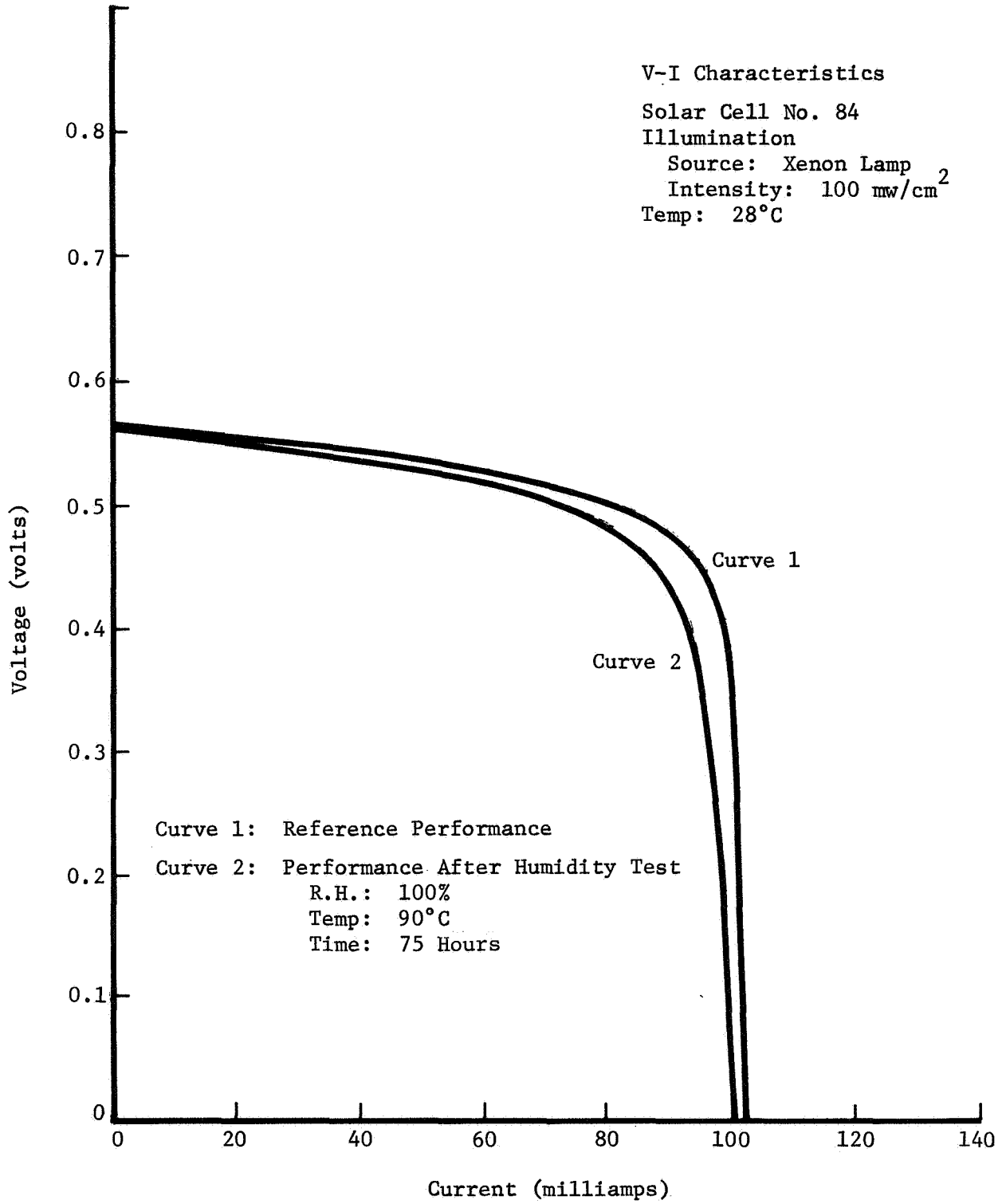
(See Page 28.)

22

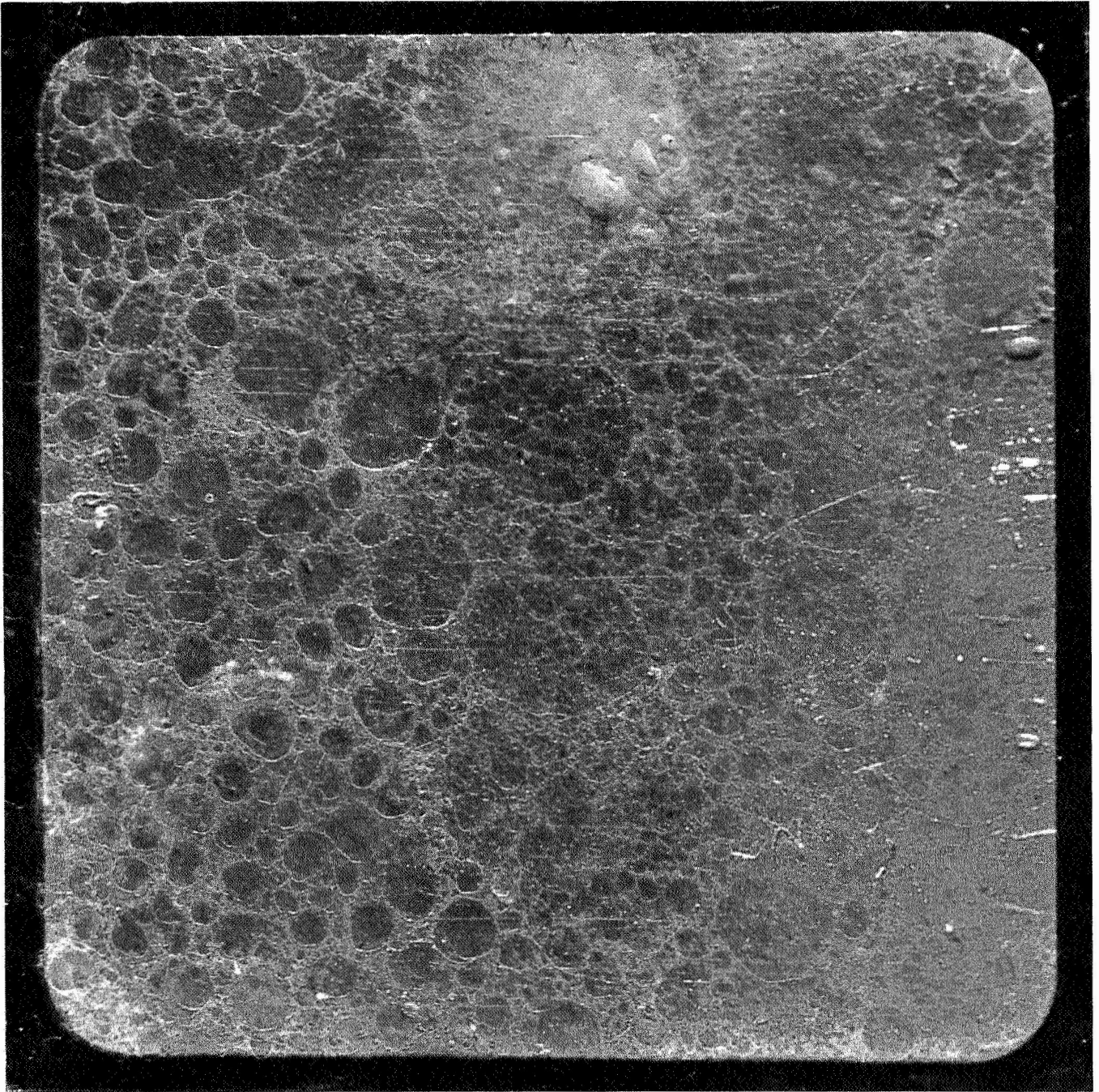Figure 15:   PERFORMANCE DEGRADATION FROM A HUMID ATMOSPHERE

Figure 16:   SOLAR CELL AFTER 75 HOURS IN HUMID ATMOSPHERE
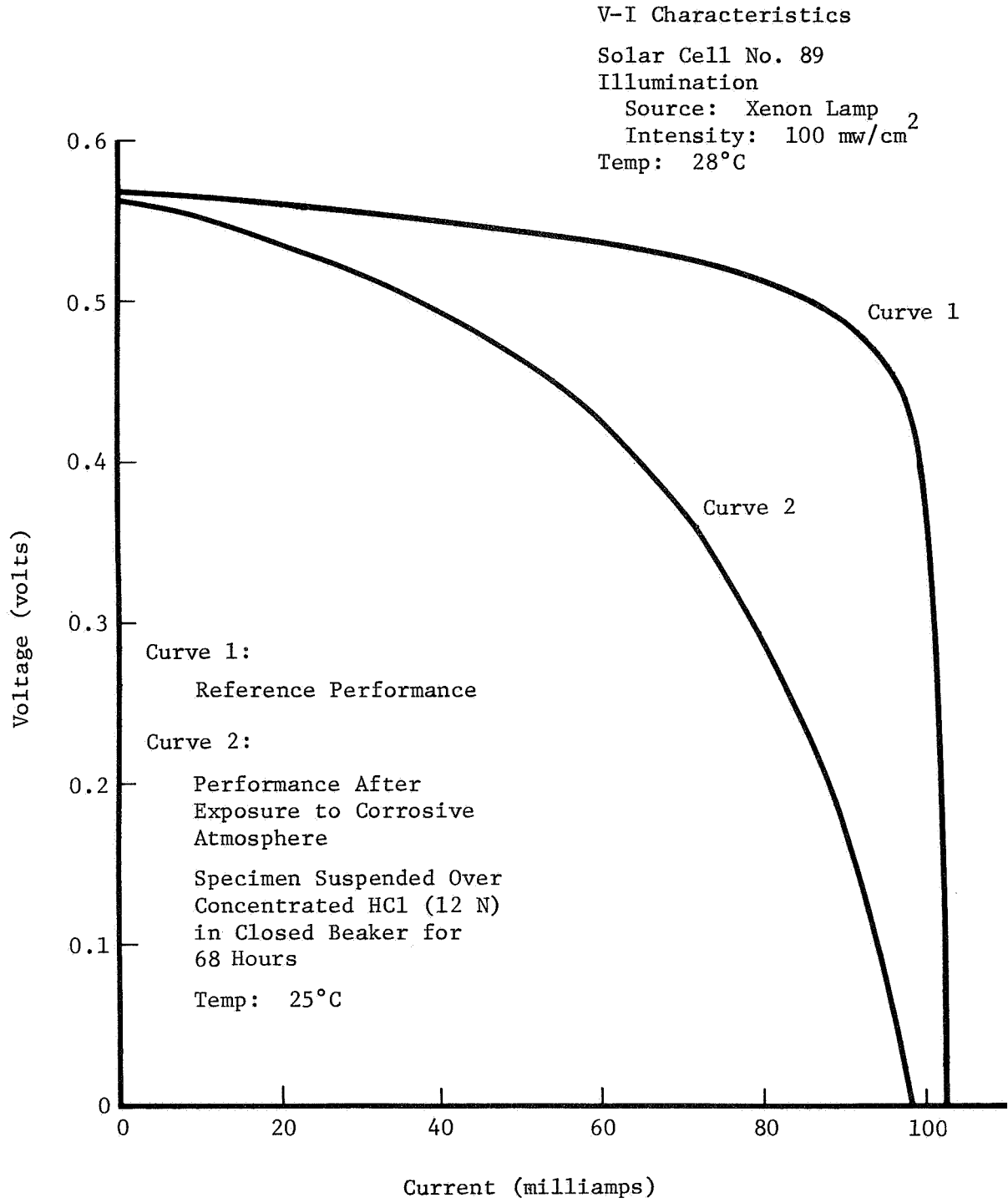
Figure 17:   PERFORMANCE DEGRADATION FROM CORROSIVE HC1 ATMOSPHERE

TIME (HOURS)	MAX PWR. (MW)	%
0	43.8	100
23	43.7	99.8
45	40.0	91.3
68	25.8	58.9

Specimen: Cell 89
Specimen Suspended Over
Concentrated HC1 (12 N)
in Closed Beaker

Temp: 25°C

Maximum Power (percent)

Time (hours)

Figure 18: PERFORMANCE DEGRADATION RATE FROM A CORROSIVE HC1 ATMOSPHERE
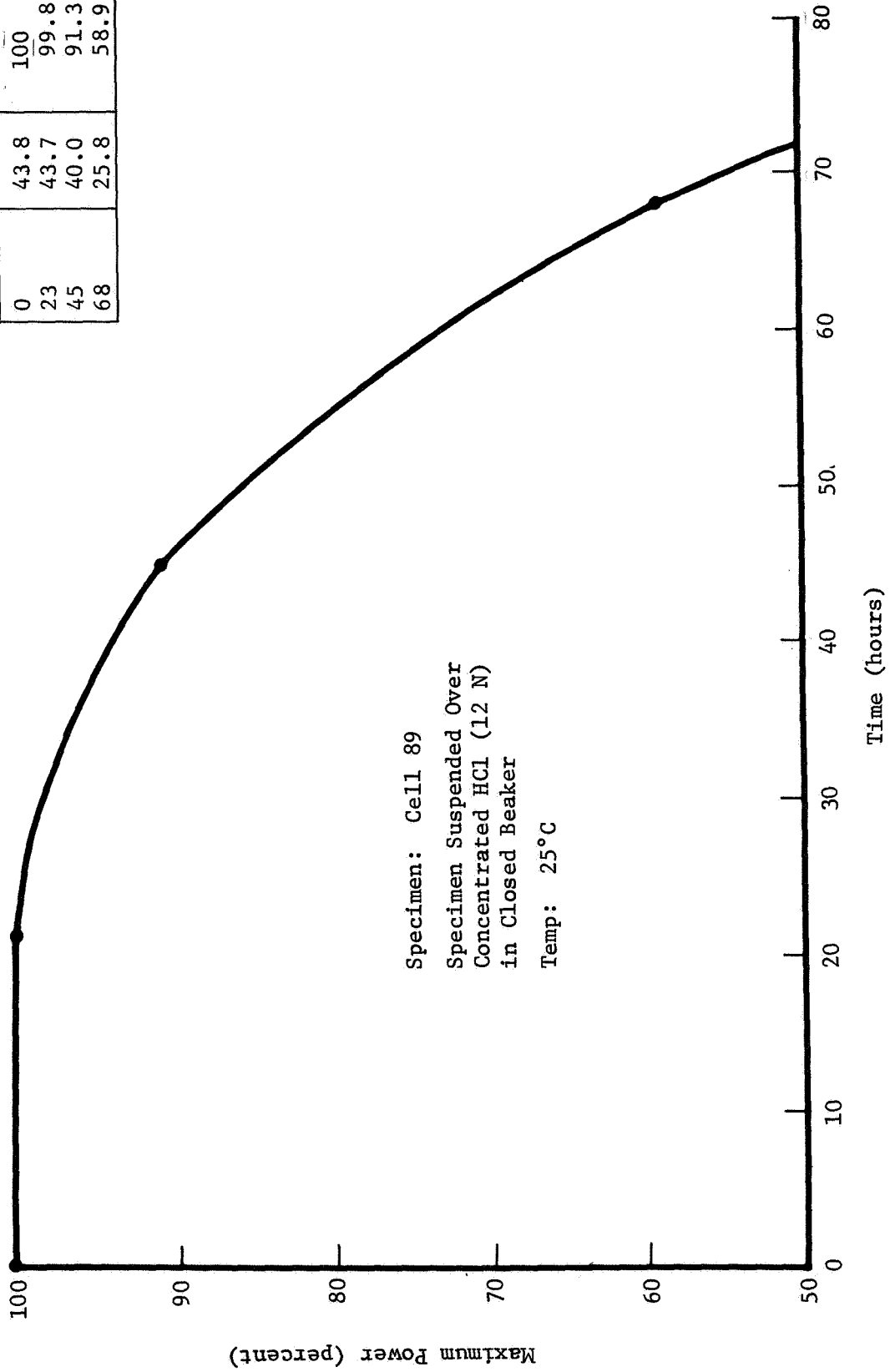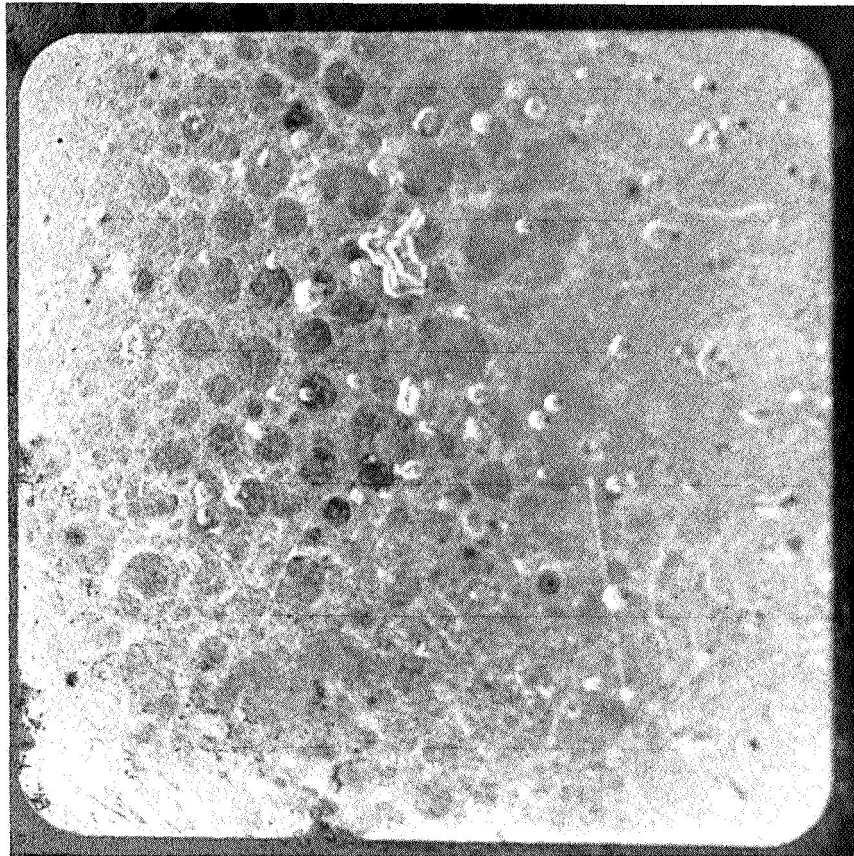
Figure 19:   SOLAR CELL AFTER 68 HOURS IN HC1 ATMOSPHERE

where R is the reaction rate
T is the temperature, $^\circ$C
k is a constant $= 10^\circ$C, approximately, for many reactions
Subscripts 1 and 2 refer to the two temperature environments.

Blistering and degradation in 100 percent relative humidity and 90°C occur in 60 to 80 hours with the cells tested. At room temperature the above equation predicts that corresponding degradation will occur at 64 X 60 = 3,840 hours or <u>160 days</u>.

It thus appears that HCl in the environment at room temperature accelerates degradation by a factor of 600. However, many electrochemical reactions do not follow the premise that the reaction rate increases a factor of two for a 10° rise in temperature. Therefore, the factor of 600 requires further confirmation.

The presence of Cl$^-$ seems to act as a catalyst in the degradation process in solar cells. 3M reports severe degradation and blistering in solar cells subjected to HF and HCl (Ref. 9). Similar tests with H_2SO_4 showed no blistering. It should be pointed out that the vapor pressure of H_2SO_4 is very low compared to that of halogen acids. At 146°C, H_2SO_4 has only a 1 mm vapor pressure so the environment about H_2SO_4 would be quite different from that about HF.

A solar cell at Boeing in a humid atmosphere with concentrated nitric acid present showed no obvious blistering after 110 hours. A V-I curve indicated degradation had occurred. However, loss of silver due to the formation of $AgNO_3$ changes the resistance of the cell and could account for the observed curve.

3.5 PHYSICAL TESTS

Characterization of the solar cell surface is a key to the understanding of the mechanism of the degradation. One model of the corrosion mechanism depends on water movement through the silver to react with titanium, but fails to explain how the highly mobile hydrogen gas is retained. One important question which may be answered with the metallographic work is how the hydrogen is trapped to form blisters. Degraded solar cells were examined by optical, mass spectroscopic, X-ray diffraction, and internal reflection spectroscopic instruments.

3.5.1 Optical and Electron Micrographs

Optical micrographs were taken with a Leitz 5mm metallograph having a 400-watt Xenon light source. The electron micrographs were taken with a JEM 7 (Jeolco) microscope using 80 kv. The specimens for electron microscopy were prepared by a two-stage technique using acetate tape (Fax film) for replicating, and using germanium and carbon for shadowing.

Blisters on solar cells are big enough to be easily seen. Figure 20 shows the appearance of the blistered surface and what appears to be a large grain size. Examination at a higher magnification shows a series of plateaus with no true grain boundary (Figures 21 and 22). Figure 22 in particular shows a continuous surface pattern through a ridge that resembles a grain boundary at low magnification. Blisters appear to be located at these plateau boundaries.

The fine-grain structure observed optically is confirmed by electron microscopy. The boundaries appear to contain a precipitate, and small pores are prevalent within the grain (Figures 23 through 25). A Texas Instruments' report interprets various grain boundary surface features as cracks (Ref. 5). The electron micrographs of surface features, as reproduced in that report, do not show enough detail to affirm the presence of cracks. Metallographic profiles will be attempted to determine whether true grains exist as outlined on the surface, and whether cracks exist along the grain boundaries. The "grains" are 4 to 9 microns in diameter and the pores are on the order of 300 angstroms (Å). The pores appear to be thermal etch pits from sintering.

3.5.2 Analysis by Mass Spectroscopy

We analyzed the constituents of blistered and nonblistered solar cell contacts using a spark-source mass spectrograph, CEC Model 21-110B. The results are below:

CONSTITUENTS OF BLISTERED CONTACT

Major 10,000 ppm	Minor 500-10,000 ppm	Lesser 10-500 ppm	Trace 1-10 ppm	Subtrace 1 ppm
Ag	Ti	F	B	S
Si	SiO	HO	P	NH_3
	SiO_2	H_2O	TiO	NH_4
		Cu	Cl	
		O	Pb	
		H	Bi	
		C	W	
			Zr	
			CF	
			CF_2	

Of most interest is the presence of 10 to 500 parts per million (ppm) F^-. This impurity must be from the etching and cleaning of the solar cell by HF. Presence of F^- may be critical to the corrosion process.

The presence of copper is expected. It is an impurity in the silver. Copper in the silver reduces silver resistance to oxidation and may affect corrosion. The carbon may be from the silicones which had been used for masking. H_2O and OH^- are attributed to moisture held in the pores and etch pits of the silver and indicate the presence of the conductive solution needed for corrosion.
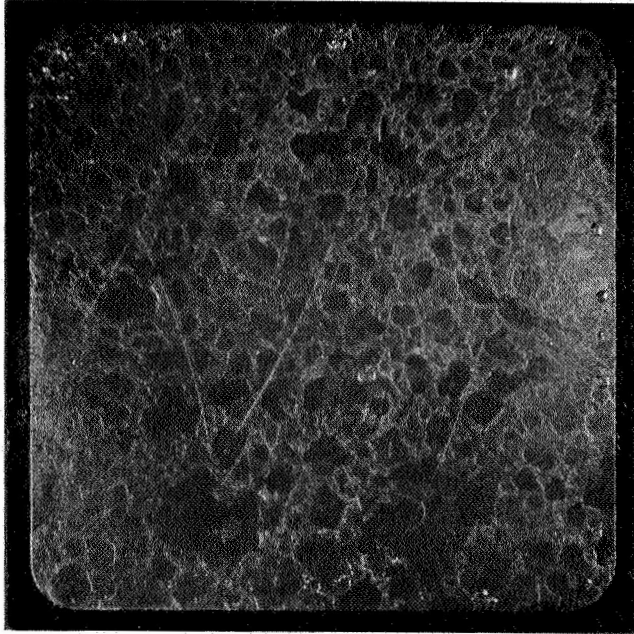
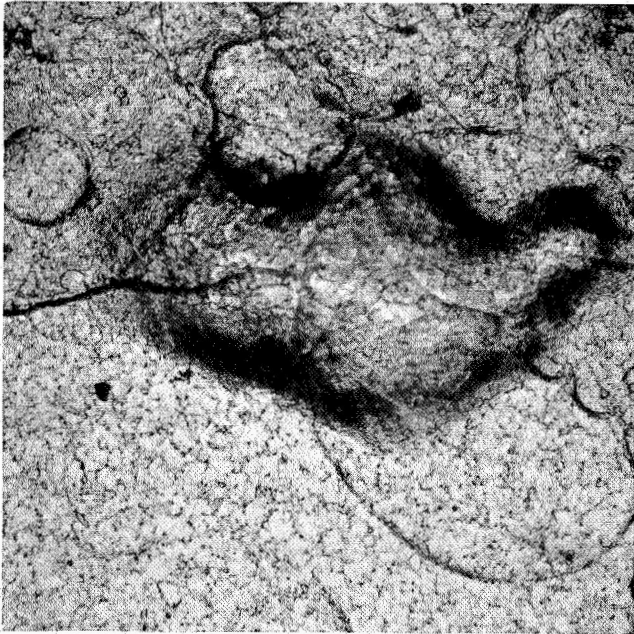Figure 20:   BLISTERED AREA, 4X MAGNIFICATION

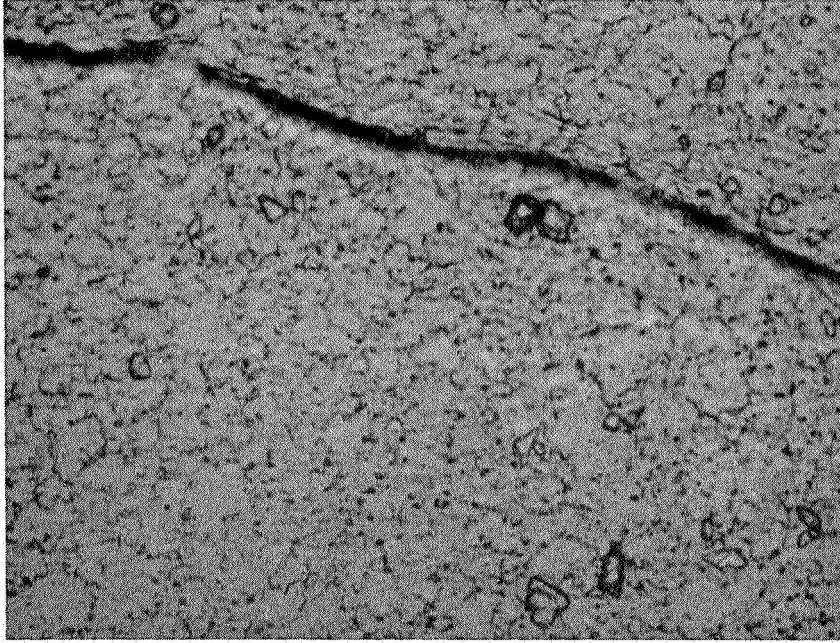Figure 21:   BLISTERED AREA, 200X MAGNIFICATION

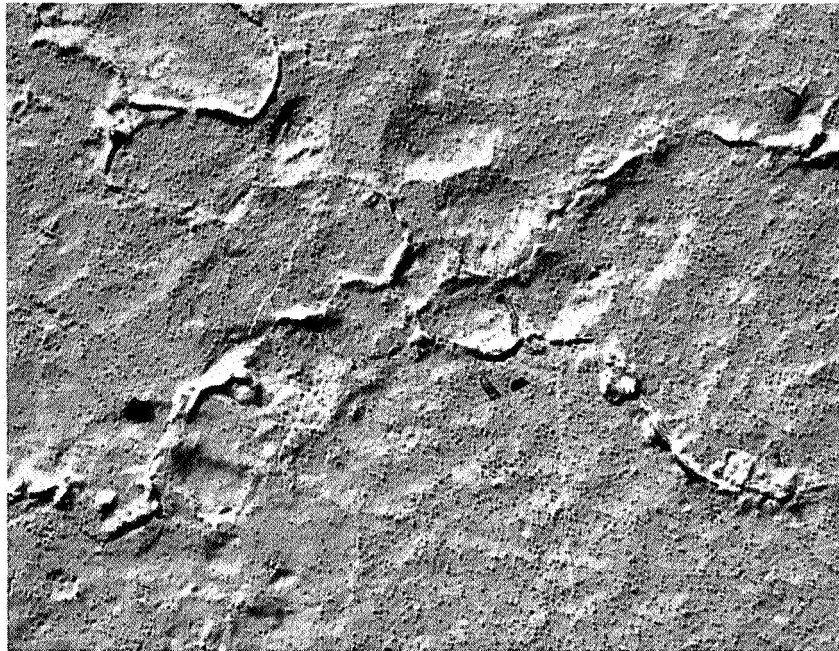Figure 22:   CELL SURFACE, 500X MAGNIFICATION

Figure 23:   ELECTRON MICROGRAPH (8000X)

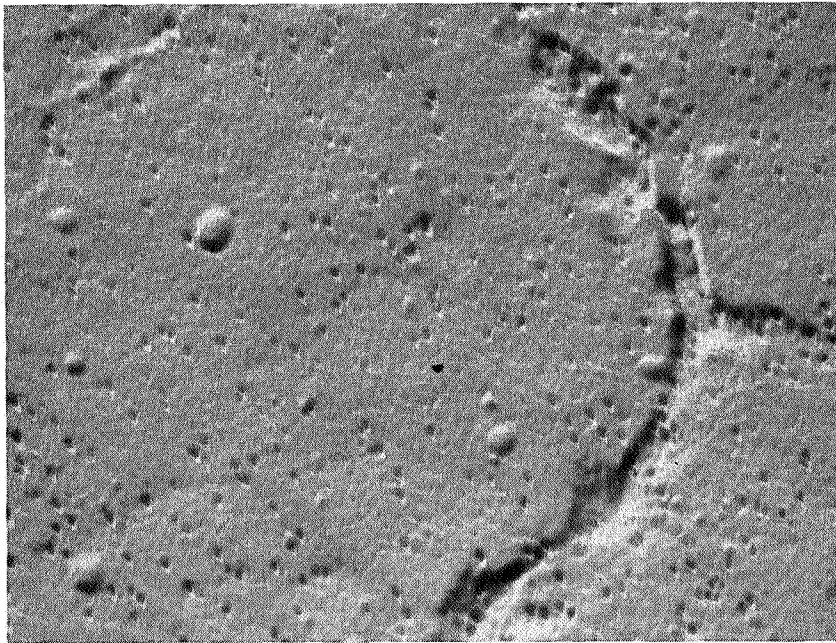Figure 24:   ELECTRON MICROGRAPH (8000X) OF SOLAR CELL SURFACE

Figure 25:   ELECTRON MICROGRAPH (31000X) OF SOLAR CELL SURFACE

Another interesting result is the presence of H_2 in larger concentrations in blistered areas compared to nonblistered areas. This is consistent with the mechanism of H_2 being formed as a product of the corrosion process.

3.5.3 Analysis of X-ray Diffraction

X-ray diffraction shows the effect of the sintering process on the surface of the silver. We see no indication that sintering introduces significant contaminants which promote corrosion. However, the surface of the silver is alternated by sintering. We do not know whether this is important in the transport of moisture or contaminants through the silver. Sintering causes partial crystallization on the surface of the silver. Scraping away the upper surface leaves a preferentially oriented silver structure. Etching away the silver layer with nitric acid reveals a crystallized layer of titanium. However, associated with the titanium-silicon interface is another layer which could not be identified with diffraction techniques. Internal reflection spectroscopy will be used to study this layer.

3.5.4 Internal Reflection Spectroscopy

Internal reflection spectroscopy takes advantages of single-crystal silicon used in the solar cell. The cell becomes a part of a prism and radiation entering the prism is reflected internally for angles of incidence greater than the critical angle (Figures 26 and 27). The beam actually penetrates slightly beyond the reflecting surface into the surface layer on the crystal. Materials on the surface will selectively absorb radiation. A plot of the attenuated radiation versus wavelength becomes an absorption spectrum characteristic of the material.

Silver-titanium contact corrosion on silicon can be examined by evaporating the desired material on the prism, conditioning the specimen, and measuring adsorption as the corrosion proceeds. Changes in the contact composition can be determined in situ with the use of a liquid sample holder (Figure 28). The depth of penetration of the beam into the contact can be controlled by the wavelength of the radiation and the angle of incidence of the radiation. Specimens have been prepared and the null measurements have been made prior to coating (Figure 29).

Internal reflection spectograms will be made after evaporating silver, titanium, and silver-titanium, using selected processes and conditioning.
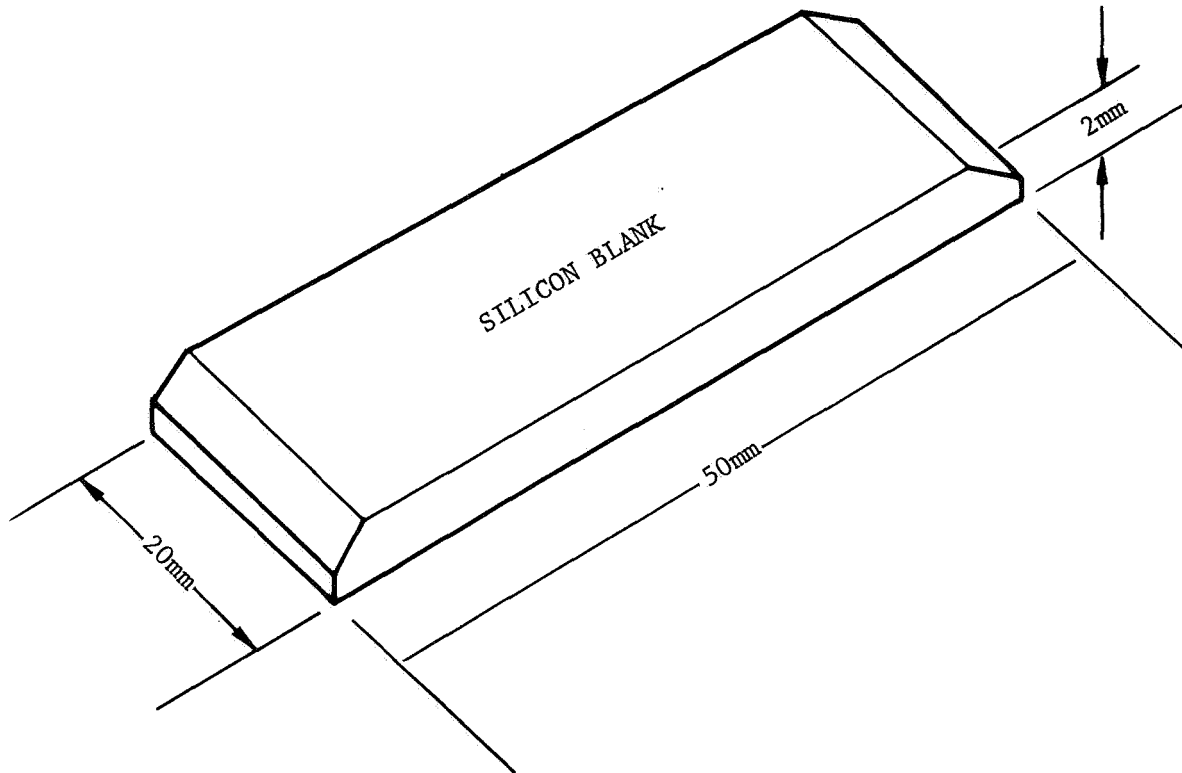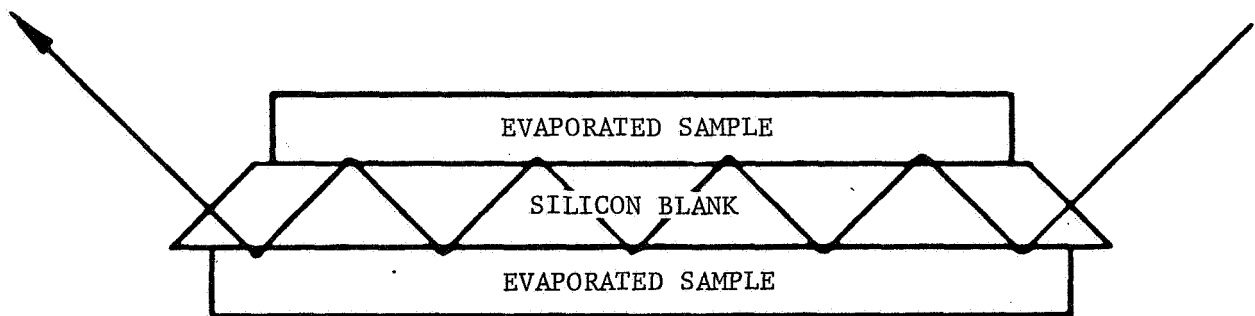
Figure 26:   INTERNAL REFLECTION SPECIMEN

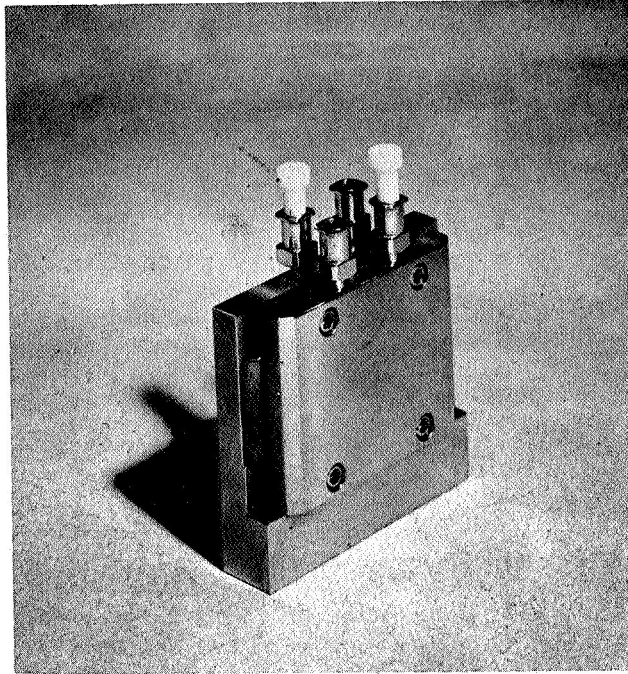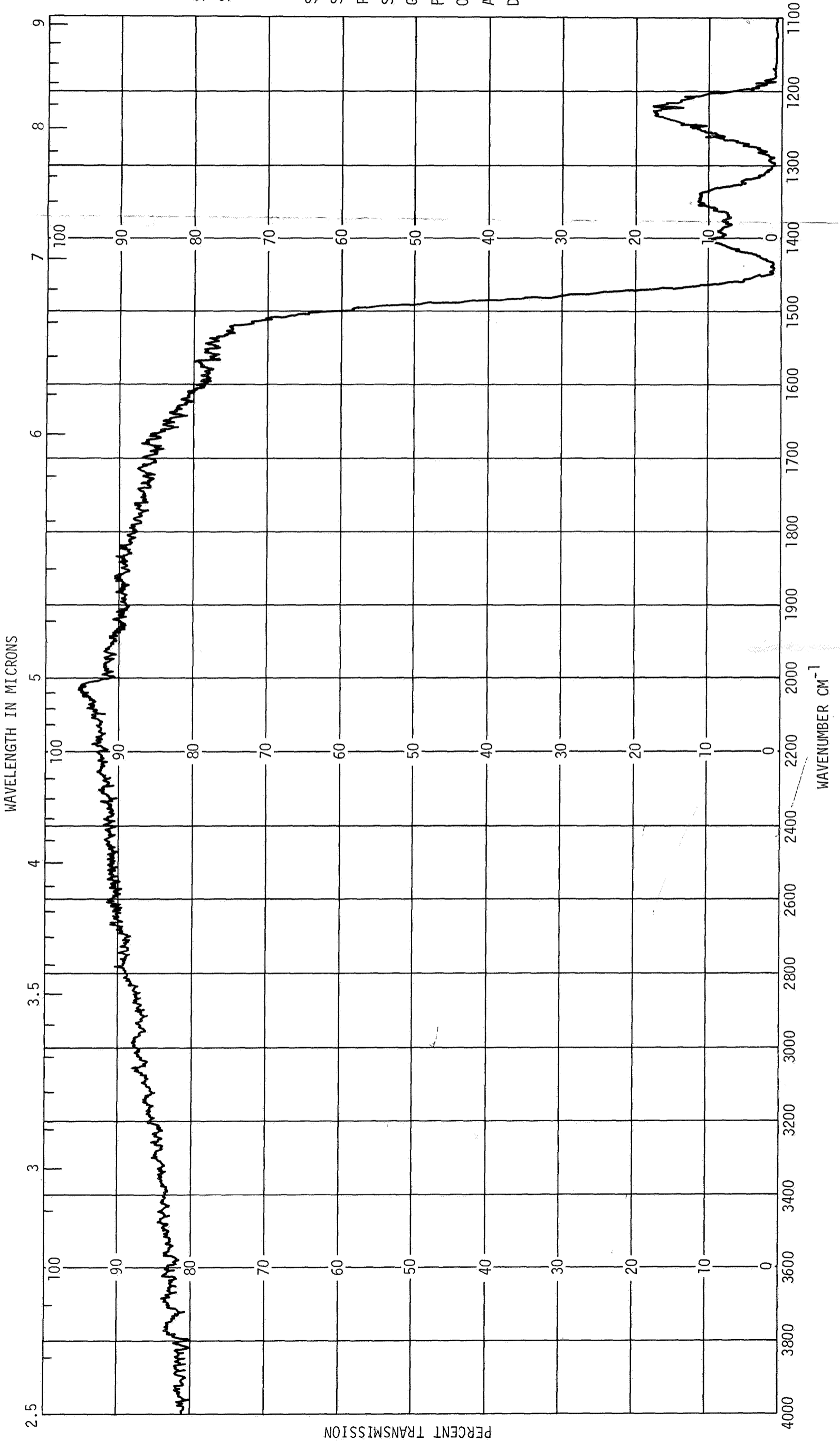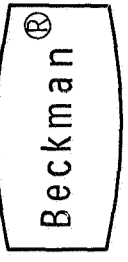Figure 27:   MULTIPLE INTERNAL REFLECTION EFFECT
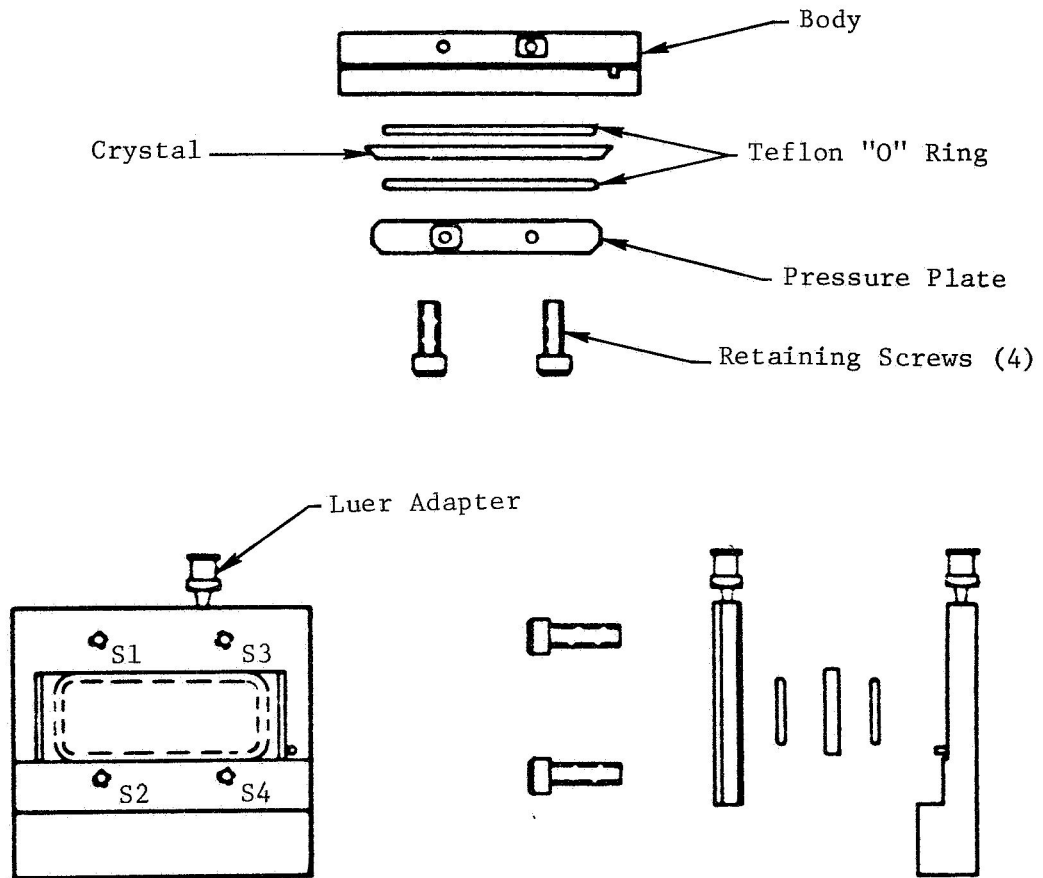
Figure 28:   LIQUID SAMPLE HOLDER

D2-126194-1

SPECTRUM NO. B

SAMPLE Silicon ATR
Crystal
Blank

SB _____ DB ╰
SB/DB ENERGY RATIO _____
RESOLUTION _____
SPEED 200 out
GAIN 3 %
PERIOD 2
ORDINATE SCALE 0-100
ANALYST _____
DATE 7/8/69

Beckman®

SPECTROPHOTOMETER

WAVELENGTH IN MICRONS

PERCENT TRANSMISSION

WAVENUMBER CM⁻¹

Figure 29: ADSORPTION SPECTRUM

36

4.0 STEPS IN MANUFACTURE OF SILICON SOLAR CELLS

Tabulated below are steps in the manufacture of a solar cell. This table, a composite of data from several sources, is useful for correlating the data from mass spectroscopy and the theoretical model. For example Step 36, cleaning in hydrofluoric acid, becomes of special interest because analysis shows that relatively large amounts of fluorides are still present on the solar-cell surface. Also, Step 53, which follows evaporation of the contacts, exposes the contact to hydrofluoric acid. Certain protective oxide coatings are known to break down when fluorides are available to take part in the reaction.

STEPS IN MANUFACTURE OF SILICON SOLAR CELLS

1. Grow ingot.
2. Clean ingot.
3. Cut flat on ingot.
4. Mount ingot for sectioning.
5. Section into disks.
6. Demount sections.
7. Production inspect sections.
8. Lap sections.
9. Mount sections for slabbing (barring).
10. Cut slabs (bars).
11. Demount slabs.
12. Lap slabs.
13. Mount slabs for slicing (wafering).
14. Mount billet in diamond-saw wafering machine.
15. Slice slab.
16. Demount slices.
17. Mount slices for polishing (alternate-etch slices).
18. Polish slices with 20 micron alumina powder.
19. Polish slices with 5 micron powder.
20. Polish slices with 1 micron powder.
21. Demount slices.
22. Production inspect slices.
23. Clean slices in trichloroethylene (alternate-acetone, isopropyl alcohol, sulfuric acid).
24. Etch slices in acid solution (acetic, nitric, hydrofluoric):

    a. Mix acetic and hydrofluoric acid and pour over slices.
    b. Add nitric acid to start etch.
    c. Etch required time, e.g., 4 minutes.
    d. Quench etch with deionized water.

25. Clean slices in deionized water.
26. Dry slices in alcohol.
27. Dry slices in stream of nitrogen gas.
28. Store in plastic containers.
29. Diffuse in quartz tube or boat with P_2O_5 carried with O_2.
30. Anneal slices.
31. Store in covered Pyrex container.
32. Mask N layer with tape (alternate-cover with wax).
33. Sandblast cells to expose p layer (alternate-chemically etch).
34. Remove mask or wax.
35. Clean cells in trichloroethylene.
36. Clean in nitric-hydrofluoric-acetic acid solution.
37. Clean in deionized water.
38. Dry with methyl or isopropyl alcohol.
39. Dry slices in stream of nitrogen gas.
40. Store slices in Pyrex container with dessicant, e.g., $CaSO_4$.
41. Load fixtures for evaporation of contacts.

42. Clean titanium filament with SiC paper.
43. Clean silver filament.
44. Measure vacuum, must be less than 5×10^{-7} Torr.
45. Evaporate titanium.
46. Evaporate titanium and silver.
47. Evaporate silver.
48. Break vacuum with dry nitrogen.
49. Place cells in sintering over.
50. Admit forming gas ($6\% H_2$ $-94\% N_2$) to oven.
51. Sinter cells at 605°C in forming gas.
52. Clamp cells between rubber wafers (alternate-mask cell faces with wax).
53. Remove N layer from cell edges with HF acid.
54. Clean cells in deionized water.
55. Evaporate silicon monoxide on cell edges.
56. Fire silicon monoxide coating.
57. Perform tape test on silver coating.
58. Clean cell after tape test.
59. Production cells mechanically.
60. Production cells electrically.
61. Store cells in polystyrene slotted boxes.
62. Package for shipment.

5.0 CONCLUSIONS

The contracted work on solar-cell contact degradation completed during the first quarter supports the following conclusions:

1) The degradation of solar cells produced in the laboratory under controlled conditions supports the postulate that the mechanism of degradation is electrochemical in nature.

2) Rest potential tests suggest that in degrading cells a second species is interacting with the silver to give a mixed rest potential which is negative with respect to the rest potential for pure silver.

3) Several environmental contaminants, such as Cl^-, F^-, OH^-, which have negative rest potentials (against SCE), produce degradation typical of that found in cells stored in industrial environments. Positive rest potentials found with solar cell-electrolyte combinations such as sulphates and nitrates do not produce typical degradation.

4) Humidity tests show that the presence of chloride ions accelerates the degradation process by several orders of magnitude over the rate in pure water vapor.

5) Preliminary physical measurements indicate that blisters are located at grain boundaries. Large quantities of H_2 were detected in the region of blisters, supporting the supposition that H_2 is released in a chemical reaction.

6.0 PROGRAM FOR NEXT QUARTER

A review of the accomplishments of the first quarter of the contracted
work indicated that the following second-quarter steps will contribute to
the objective of understanding the mechanism of silver-titanium contact
degradation:

1) Continue potentiostatic and rest-potential measurements.

2) Relate the contact degradation to the materials and processes used
    in the manufacture of solar cells. The mass spectroscopy results
    indicate several contaminating ions are present in the cell.
    Examples are F^-, Cu^{++}, Cl^-. The questions to be answered are:
    What contaminants promote degradation? How do the reaction rates
    compare for the various contaminants? What are the critical con-
    centrations necessary for active corrosion?

3) Study the transport of water and H_2 through the silver layer using
    internal reflection spectroscopy, and possibly radioactive tracers.
    Resolve the question: If water can get through the Ag layer, why
    cannot H_2 be released readily?

BIBLIOGRAPHY

1. Significant contributions to this report were made by T. R. Beck and C. J. Bishop.

2. R. Jacobson, *Solar Cell Contact Development,* First Quarterly Report, Contract No. NAS 5-11595, Goddard Space Flight Center (Sept. 1968).

3. R. Jacobson, *Solar Cell Contact Development,* Second Quarterly Report, Contract No. NAS 5-11595, Goddard Space Flight Center (Dec. 1968).

4. A. W. Adamson, Physical Chemistry of Surfaces, 2nd Ed. (Interscience, New York, 1967), p 58.

5. G. Morrison, *Solar Cell Contact Deposition Parameter Study,* First Quarterly Report, Contract No. NAS 5-11612, Goddard Space Flight Center (Nov. 1968).

6. M. Lepselter, private communication.

7. M. Pourbaix, Atlas of Electrochemical Equilibria in Aqueous Solutions (Pergamon Press, New York, 1966) p 213 and p 393.

8. F. H. Uhlig, Corrosion and Corrosion Control (John Wiley, New York, 1963), p 70.

9. R. Jacobson, *Solar Cell Contact Development,* Third Quarterly Report, Contract No. NAS 5-11595, Goddard Space Flight Center (March 1969).